Hybrid Additive Manufacturing of a Topologically Optimized, Modular Lattice Wheel for Terrain-Adaptive Mobility on Martian Surfaces

Jubel Kurian[1], Maheep Bubna[2], Morey Levy[3], and Zach Caicedo[4]
Virginia Tech, Blacksburg, VA, 24061, United States of America

Mobility on the Martian surface poses complex challenges due to abrasive regolith, thermal cycling, low atmospheric pressure, and unpredictable terrain. To address these, this study presents the design, development, and validation of a hybrid-manufactured, terrain-adaptive Mars rover wheel. The final architecture integrates a CNC-machined titanium skeleton, a topology-optimized titanium lattice core fabricated via Laser Powder Bed Fusion (LPBF), and modular tread lugs constructed from flexible TPU using material extrusion. Each component is functionally partitioned to optimize structural integrity, impact absorption, and adaptability while ensuring repairability and manufacturability in both Earth-based and potential in-situ environments. A structured design process incorporating Quality Function Deployment (QFD), Design for Additive Manufacturing (DfAM), and lattice benchmarking led to the selection of the Octa-Hedroid lattice topology for the TPU tread lugs. Finite element analyses showed that this structure minimizes deflection (0.57 mm) and maintains low von Mises stress (15 MPa), while also promoting self-cleaning under Martian conditions due to its open, interconnected void geometry. Prototype fabrication at both 1:2 and 1:1 scales validated printability, modular assembly, and robustness under thermal, impact, and rolling resistance tests across multiple terrains. This work demonstrates how hybrid additive manufacturing can be strategically employed to meet planetary mobility needs through weight-efficient, compliant, and serviceable designs. The modular lattice-based wheel provides a scalable and maintainable alternative to traditional rigid or mesh-based rover wheels, with significant promise for deployment in future Mars or other extra-terrestrial exploration missions.

[1] Ph.D Candidate, Kevin T. Crofton Department of Aerospace and Ocean Engineering, Virginia Tech, AIAA Student Member
[2] Graduate Student, Department of Mechanical Engineering, Virginia Tech
[3] Undergraduate Student, Department of Mechanical Engineering, Virginia Tech
[4] Undergraduate Student, Department of Mechanical Engineering, Virginia Tech

Nomenclature

AM	Additive Manufacturing
CAD	Computer-Aided Design
CNC	Computer Numerical Control
DfAM	Design for Additive Manufacturing
ESA	European Space Agency
EVA	Extravehicular Activity
FEA	Finite Element Analysis
FDM	Fused Deposition Modeling
FOS	Factor of Safety
HIP	Hot Isostatic Pressing
LPBF	Laser Powder Bed Fusion
ME	Material Extrusion
NASA	National Aeronautics and Space Administration
PLA	Polylactic Acid
QFD	Quality Function Deployment
SLM	Selective Laser Melting
TPU	Thermoplastic Polyurethane

I. Introduction

A. Problem Definition and Motivation

The continued exploration of extra-terrestrial bodies such as Mars, the Moon, and potentially Europa or Titan, requires robotic and crewed rovers that are not only highly capable in their scientific instrumentation but also exceptionally robust in terms of mechanical mobility. The terrain on these celestial bodies is characterized by a combination of loose regolith, sharp rocks, steep inclines, and unpredictable subsurface conditions. The Martian surface, for example, comprises basaltic rock fragments, fine dust, and compacted soil that present major traversal challenges, especially over extended periods and without the benefit of terrain maintenance or repair facilities.

Historically, rovers like Spirit, Opportunity, Curiosity, and Perseverance have relied on rigid aluminum alloy wheels with grousers (cleats) to gain traction [1][2]. However, mission logs and post-mission analysis have reported structural fatigue, wheel surface punctures, and deformation from extended travel, especially over sharp rock formations like the "ventifacts" encountered by Curiosity[3]. These failures directly impact mission life, as the rover's scientific objectives can only be met if mobility is preserved over thousands of terrain maneuvers.

On Earth, mobility systems typically rely on pressurized pneumatic tires for traversing uneven terrain, thanks to their ability to passively absorb shocks, deform around obstacles, and maintain high traction through inflation-controlled stiffness. However, this terrestrial solution is fundamentally incompatible with extra-terrestrial applications due to several non-negotiable limitations:

- Atmospheric Absence: Mars has a surface pressure of ~600 Pa (0.6 kPa), less than 1% of Earth's sea-level pressure [4]. Pneumatic tires rely on internal gas pressure being significantly higher than ambient pressure. In Martian conditions, this pressure differential would pose catastrophic risks for explosion or leakage even with minor punctures.
- Temperature Extremes: Martian surface temperatures fluctuate heavily. This temperature cycling results in volumetric expansion and contraction of gases, leading to pressure instability and potential failure in sealed pneumatic systems.
- Abrasive and Sharp Regolith: Martian soil particles have not undergone the kind of erosive weathering seen on Earth, making them jagged and highly abrasive. This increases the likelihood of puncturing a pressurized tire, which cannot be repaired remotely.
- Operational Lifetime Requirements: With rover missions lasting several years, reliability and maintainability are critical. A puncture or deformation in a pneumatic tire mid-mission could render the entire rover immobile.

In response to these factors, space agencies have pivoted toward non-pneumatic, structurally compliant wheels that integrate passive terrain adaptability within the material and geometry of the wheel itself. NASA's Spring Tire concept developed in collaboration with Goodyear is a prime example, leveraging shape-memory alloys to provide resilience and flexibility [5]. This project is motivated by the need to develop an innovative, flexible, and manufacturable Mars rover wheel that addresses these limitations while remaining lightweight, repairable, and compliant with rough terrain. This project also aims to develop a design that is easily repairable and can be manufactured easily on Mars. Unlike traditional rigid wheels or experimental metal mesh tires, the proposed wheel is based on a hybrid 3D lattice structure that combines the mechanical resilience of titanium with the terrain-conforming ability of polymeric tread structures. The motivation extends beyond functionality to also explore the manufacturability, cost-efficiency, and scalability of such designs using modern additive and subtractive manufacturing techniques.

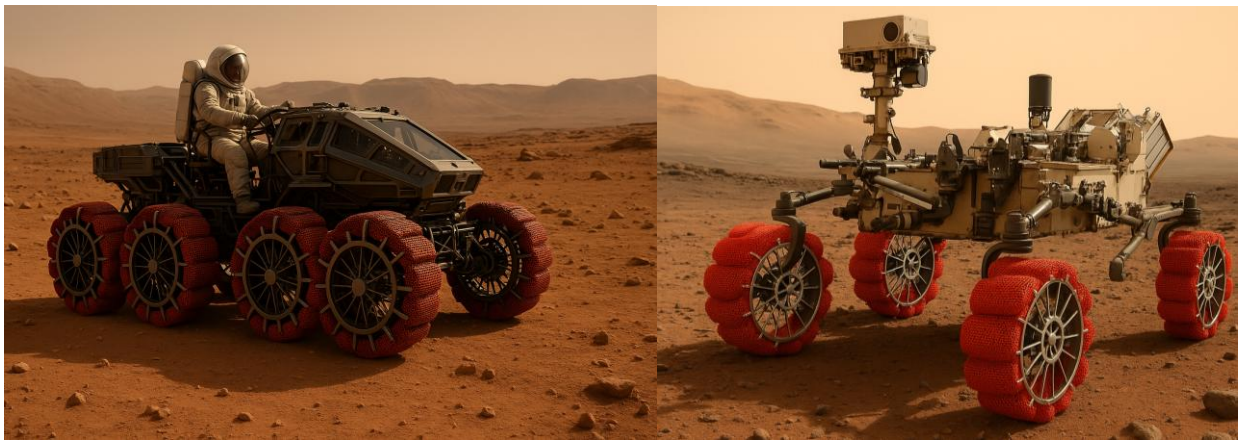

Figure 1: (a) AI render of the lattice-based wheel design developed by the team on an extraterrestrial human-operated vehicle. (b) AI render of the lattice-based, scaled-down wheel design developed by the team on a rover.

B. Problem Scoping

The current work aims to develop and analyze a scaled-down prototype of a flexible, hybrid-manufactured Mars rover wheel optimized for passive compliance, energy absorption, terrain adaptability, and modular maintenance. The design incorporates a multi-material construction with each material serving a specific structural and functional role within the wheel:

- Titanium alloy skeleton for strength and stability
- Topology-optimized lattice structures for impact dissipation and reduced weight
- Flexible TPU tread modules for traction and ground interaction

The scope of this study includes:

- Customer need identification and prioritization via QFD and pairwise comparison
- CAD modeling of the full wheel system including modular tread elements
- Material selection and justification based on mechanical, thermal, and chemical properties.
- Hybrid manufacturing strategy development.
- Machine and process down-selection for both prototyping and future deployment
- FEA (Finite Element Analysis) analysis on the manufactured prototype designs
- Evaluation of manufacturing feasibility at Earth-based academic facilities

Out-of-Scope Considerations

Given the constraints of time, budget, and academic prototyping limitations, several aspects are acknowledged as outside the scope of this study but critical for eventual Mars deployment:

- The final design will need a scaled-up model based on the loading and chassis structure requirements
- Full-scale testing under Martian atmospheric and thermal conditions
- Dust abrasion life-cycle studies, which would simulate repeated exposure to fine-grain Martian regolith under low-pressure
- Thermal cycling tests to verify material integrity
- Rover integration and drive-system interfacing (Example: Rocker Boogie mechanism)
- Autonomous damage detection, lug replacement, or terrain-adaptive control algorithms

Additionally, while the current prototype utilizes a Shore 90A TPU suitable for Earth-based testing, a Martian application would require an upgraded elastomer such as Shore 75D TPU with UV stabilizers, cryogenic resilience

additives, and anti-static properties to prevent dust accumulation and electrostatic discharge [6]. This final design represents a functional prototype for conceptual validation and testing. For Martian deployment, the design would need to be scaled up, fabricated with aerospace-certified materials, and subjected to space-qualification protocols under NASA or ESA standards.

C. AM Rationale

The selection of **Additive Manufacturing (AM)** for both the metallic and polymeric components of the Mars rover wheel is based on its ability to address specific geometric, functional, and operational demands that are unattainable or highly inefficient with traditional manufacturing methods. The wheel incorporates a hybrid construction of metallic load-bearing components and flexible traction modules, each with highly specialized geometries that demand advanced fabrication capabilities.

To achieve this, two complementary AM technologies are used:

- **Laser Powder Bed Fusion (LPBF)** for titanium components
- **Material Extrusion (ME)** for TPU components

a. AM Rationale for using ME for the TPU Components:

The outer tread modules are designed with complex 3D lattice geometries that deliver passive compliance, debris-shedding capability, and high surface adaptability. These performance characteristics demand a high degree of geometric control, material customization, and modularity, all of which are best delivered through Material Extrusion (ME).

1. **Complex Lattice Geometries**
   The tread design requires intricate internal lattice structures to enhance shock absorption, flexibility, and self-cleaning behavior. Such fine, structured porosity is not manufacturable through injection molding or casting without expensive, multi-part molds or sacrificial cores. ME enables layer-by-layer fabrication of voided, functionally tuned geometries without support tooling.
2. **Modular and Distributed Fabrication**
   AM allows the fabrication of modular components, enabling localized reprinting and replacement of individual tread units. This modularity supports design variations, replacement logistics, and failure redundancy that are impractical with monolithic molded or cast components.
3. **Rapid Iteration and Customization**
   During the prototyping phase, AM enables quick design changes and testing cycles without requiring new tooling. This drastically reduces turnaround time, enabling design-for-performance cycles ideal for R&D and future mission-specific tuning.
4. **In-Situ Manufacturing and Repair on Mars**
   ME systems are portable, low-power, and mechanically simple, making them suitable for deployment on Mars. By transporting feedstock (e.g., TPU spools), astronauts or robotic systems can fabricate or repair tread modules on-demand, reducing spares inventory and launch mass. This capability also supports in-situ adaptability to unexpected terrain challenges.
5. **Scalability and Redundancy**
   AM allows parallel production of multiple lugs on a single print bed, offering scalability for high-volume fabrication or reconfiguration during extended missions. Damaged parts can be selectively reprinted, without the need to remanufacture the entire wheel.
6. **Support for Functional Grading**
   ME allows variation in infill density and wall thickness throughout the part. This enables the design of tread modules with site-specific stiffness and damping, offering performance gradients that cannot be achieved through homogeneous molding techniques.

b. AM Rationale for using LPBF for the Titanium Components:

The structural core of the wheel, including the hub, outer rim, and internal lattice, leverages LPBF to fabricate geometrically optimized metallic components. These parts are subject to multi-axial loading, require precise topology control, and must minimize mass while maintaining structural integrity.

1. **Topology Optimization Realization**
   The internal lattice structure is the result of a topology optimization process aimed at minimizing weight while maintaining load paths for torque transmission and shock absorption. LPBF uniquely allows the manufacture of these complex, stress-optimized geometries without requiring assembly or multi-part welding.
2. **Geometrical Freedom**
   LPBF supports overhangs, internal channels, and closed-cell lattice features that are infeasible with CNC machining or casting. This capability allows for material placement only where needed, resulting in significant mass savings without sacrificing performance.
3. **Consolidated Part Manufacturing**
   LPBF enables the integration of multiple functional features into a single monolithic component, reducing part count, fasteners, and assembly steps. This not only improves mechanical robustness but also reduces failure risk associated with joints and interfaces.
4. **Near-Net-Shape Production**
   LPBF delivers parts with minimal material waste, especially valuable for high-cost alloys like titanium. While subtractive machining discards a large fraction of material, LPBF minimizes waste and reduces post-processing requirements to only critical surfaces.
5. **High Precision for Interface Fit**
   LPBF components, followed by targeted machining at interfaces (e.g., hub bore, axle mounts), enable high-tolerance mating features, sufficient for functional integration with bearings, dowels, or suspension systems.
6. **Internal Feature Access and Sealing**
   LPBF allows creation of sealed or enclosed internal lattice structures for shock management and thermal modulation. These cannot be machined or cast without multi-part tooling or complex post-processing.
7. **Manufacturing Efficiency for Low Volumes**
   Traditional methods (e.g., forging or casting) are cost-effective only at high volumes due to mold/tooling costs. LPBF is ideal for low-volume, high-performance applications such as planetary rover components where every unit is custom or mission-specific.
8. **Future Compatibility with In-Situ Metal Printing**
   LPBF technology is increasingly being adapted for in-situ metal additive manufacturing in space or on lunar/Martian surfaces. Developing components with LPBF today prepares the design pipeline for eventual insitu-compatible fabrication, aligning with long-term planetary manufacturing goals.

II. Customer Needs and Specifications

A. Customer Needs

The design of the flexible lattice rover wheel is driven by a set of well-defined customer needs that reflect the operational demands of extraterrestrial exploration. These needs ensure the wheel performs reliably under extreme environmental and mechanical conditions, while aligning with industrial constraints. **Key customer needs** include:

- Durability – ensuring long-term performance under extreme Martian conditions
- Adaptability/Navigability – enabling movement across varied and unpredictable terrain
- Lightweight – minimizing mass to reduce launch and operational costs
- Traction – improving grip and stability on loose or uneven Martian surfaces
- Manufacturability – allowing for efficient and feasible production processes
- Compatibility – ensuring integration with existing rocker-bogie suspension systems

- Low Cost – maintaining budget awareness, though less critical in space applications

The above-mentioned 'key needs', in addition to a couple more secondary needs, can be classified into four main categories - Product, Process, Material, and System Integration and Logistical needs, in order to ensure clarity in design translation.

a. **Product Needs:** These define the core performance and operational characteristics expected from the final product.

   1. Durability: The wheel must withstand repeated mechanical loading, impact events, and abrasive Martian terrain without structural failure.
   2. Terrain Adaptability: The design must enable effective traversal across soft regolith, sharp rocks, inclines, and variable terrain.
   3. Traction: The wheel must maintain consistent ground engagement to prevent slippage and ensure mobility on loose soil.
   4. Weight Minimization: Total wheel mass must be kept low to reduce launch costs and preserve rover energy efficiency.
   5. Modularity and Replaceability: Tread elements or spokes should be individually replaceable to support in-field repairs.
   6. Redundancy: Wheel should retain function despite partial damage (e.g., broken spokes or worn tread).
   7. Shock Absorption: The design must dampen terrain-induced vibrations to protect internal payloads and sensors.

b. **Process Needs:** These focus on the manufacturability, repeatability, and feasibility of producing the wheel using Earth-based and potentially in-situ fabrication methods.

   1. Prototyping Agility: The design should allow for rapid prototyping using university-available AM systems.
   2. Manufacturability at Scale: The design must be suitable for limited-scale production with minimal post-processing, using available industrial AM/CNC systems.
   3. Ease of Assembly: The modular components must interface reliably without precision alignment tools.
   4. Repairability: The design must allow segment-level disassembly and replacement with minimal tools.

c. **Material Needs:** These concern the mechanical, environmental, and operational properties of selected materials.

   1. High Strength-to-Weight Ratio: Structural materials must be lightweight yet capable of bearing rover loads and resisting failure.
   2. Thermal Stability: Materials must retain mechanical properties under Martian temperature cycles.
   3. UV and Dust Resistance: Surface materials must survive exposure to high UV levels and abrasive regolith.
   4. Compatibility with AM: Chosen materials must be printable using LPBF (Ti) or ME (TPU), and allow tuning of microstructure or stiffness.

d. **System Integration and Logistical Needs:** These needs relate to how well the wheel design interfaces with other rover systems, launch vehicle constraints, and planetary deployment processes.

   1. Volume Efficiency / Packaging Fit: The wheel should conform to the dimensional and stowage constraints of rover launch configurations (e.g., within an aeroshell or compact transport module).
   2. Interface Compatibility: The hub and mounting points must be compatible with the rover's suspension system (e.g., rocker-bogie arms), including torque transmission and load path alignment.
   3. Mass Constraints: Wheel mass must remain within mission-specific mass budgets for launch vehicle payload allocation.
   4. Thermal Interface Readiness: The wheel must not interfere with nearby radiators, heaters, or dust protection systems.

5. Deployment Readiness: The wheel must require minimal on-site assembly post-landing (ideally pre-integrated or robotically deployable).
6. Storage Survivability: The design should withstand mechanical stresses and vibrations during launch, landing, and transit.

B. Specifications and Quality Function Deployment (QFD) Chart

While taking every single possible customer need into consideration, the technical '**key needs**' as mentioned at the beginning of the last section were identified to be mission-critical and within the scope of this project for this class. Based on these 'key needs', to ensure the design meets the needs and expectations of stakeholders, a quality function deployment (QFD) analysis is conducted to systematically translate customer needs into measurable engineering specifications. This process supports informed AM selection by identifying key performance metrics and ranking them based on technical importance and difficulty. The team identified nine specifications to help quantitatively evaluate our concept and AM process, as mentioned in the 'key needs'. The team included these nine specifications in the QFD, as seen in Figure 1, which include: weight, tensile strength, manufacturability of the prototype, manufacturability of the final product, traction effectiveness surface finish, flexural modulus, environmental sustainability, and design adaptability.

Based on the QFD chart below, the team should prioritize specifications such as weight, tensile strength, traction effectiveness, flexural modulus, and design adaptability, as these demonstrate high importance and may be easier to achieve. In contrast, less emphasis should be placed on factors like prototype manufacturability, surface finish, and flexural modulus, as they are either more difficult to quantify or contribute less significantly to overall performance goals.

To evaluate and prioritize the customer needs for the Mars rover wheel, a pairwise comparison method was employed as depicted in Table 1. This method involves systematically comparing each need against the others to determine its relative importance in the context of extraterrestrial vehicle performance. Each comparison was scored using a scale where a value of 1 indicates greater importance, 0.5 indicates equal importance, and 0 indicates lesser importance. The needs evaluated included durability, adaptability, weight, traction, manufacturability, compatibility, and cost.

Table 1: Pairwise Comparison of Customer Needs

	Durability	Adaptability	Weight	Traction	Manufacturability	Compatability	Cost	SUM	WEIGHT	Customer Need	Relative Weight	Rank
Durability		1	1	1	1	1	1	6.0	0.2857	Durability	28.57%	1
Adaptability	0		0.5	0.5	0.5	1	1	3.5	0.1667	Adaptability	16.67%	3
Weight	0	0.5		0.5	0.5	1	1	3.5	0.1667	Weight	16.67%	3
Traction	0	0.5	0.5		1	1	1	4.0	0.1905	Traction	19.05%	2
Manufacturability	0	0.5	0.5	0		1	1	3.0	0.1429	Manufacturability	14.29%	5
Compatability	0	0	0	0	0		1	1.0	0.0476	Compatability	4.76%	6
Cost	0	0	0	0	0	0		0.0	0.0000	Cost	0.00%	7

		Importance (Customer Needs)	SPECIFICATIONS:	Weight	Tensile Stength	Manufacturability (Prototype)	Manufacturability (Final)	Traction Effectiveness	Surface Finish	Flexural Modulus	Environmental Sustainability	Design Adaptability
				1	2	3	5	6	7		8	9
	Direction of Improvement			↓	↑	↑	↑	↑	↑	◯	↑	↑
#	CUSTOMER NEEDS:											
1	Lightweight	16.67%		5	3	3	3			3		3
2	Durable	28.57%		3	5			1		5	3	3
3	Adaptability & Navagability	16.67%		2	4			4	4	3	5	5
4	Low Cost	0.00%		2	2	4	4	2	4	4	3	4
5	Compatability	4.76%		1		2	2	1	2		3	
6	Traction	19.05%			1			5	5		4	4
7	Manufacturability	14.29%		2	2	5	5	3	4	3		3
	TECHNICAL IMPORTANCE, DIFFICULTY, AND PRIORITY:											
	Technical importance (calculated, absolute)			2.36	3.07	1.31	1.31	2.38	2.29	2.86	2.60	3.38
	Technical importance (calculated, percentage)			10.9%	14.3%	6.1%	6.1%	11.0%	10.6%	13.3%	12.0%	15.7%
	Technical importance (calculated, rank)			6	2	8	8	5	7	3	4	1
				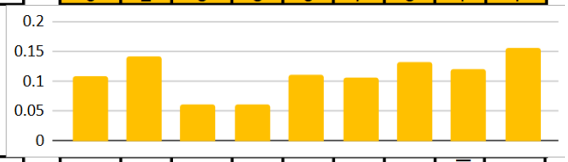								
	Units			kg	MPa	1-5	1-5	H/M/L	1-5	GPa	Pass/Fail	1-5
	Marginal Target Value			<9	<245	>3	>3	Med	>2	<1.5	Pass	>3
	Ideal Target Value			<8	>245	>4	>4	High	>3	<1.15	Pass	>4
	Technical Difficulty			3	2	1	3	4	1	5	2	4
	Technical Priority (calculated)			7.072	6.143	1.309	8.929	4.525	2.286	4.285	6.190	3.525
	Technical Priority (calculated, rank)			4	5	9	7	3	8	1	6	2
				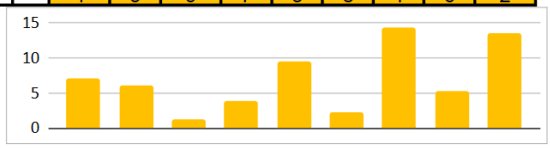								

Figure 1: Quality Function Deployment

From this analysis, durability emerged as the most critical requirement, scoring 28.57% of the total importance weight. This reflects the necessity for the wheel to withstand extreme Martian terrain over long missions. Traction (19.05%) and adaptability (16.67%) were also ranked highly, highlighting the need for consistent ground contact and the ability to deform appropriately to terrain irregularities. Weight and manufacturability followed closely, recognizing the constraints of payload efficiency and iterative prototyping. Interestingly, compatibility and cost were assigned lower weights, suggesting that performance and functionality are prioritized over economic or integration concerns in the context of mission-critical components. As industry research standards, the cost of a component is usually high due to the high-end engineering nature of the work. Hence, low priority to the cost involved is acceptable for the current study; however, as the design matures, the cost aspect can be improved significantly. This prioritization formed the basis for translating customer needs into measurable engineering specifications via the QFD approach.

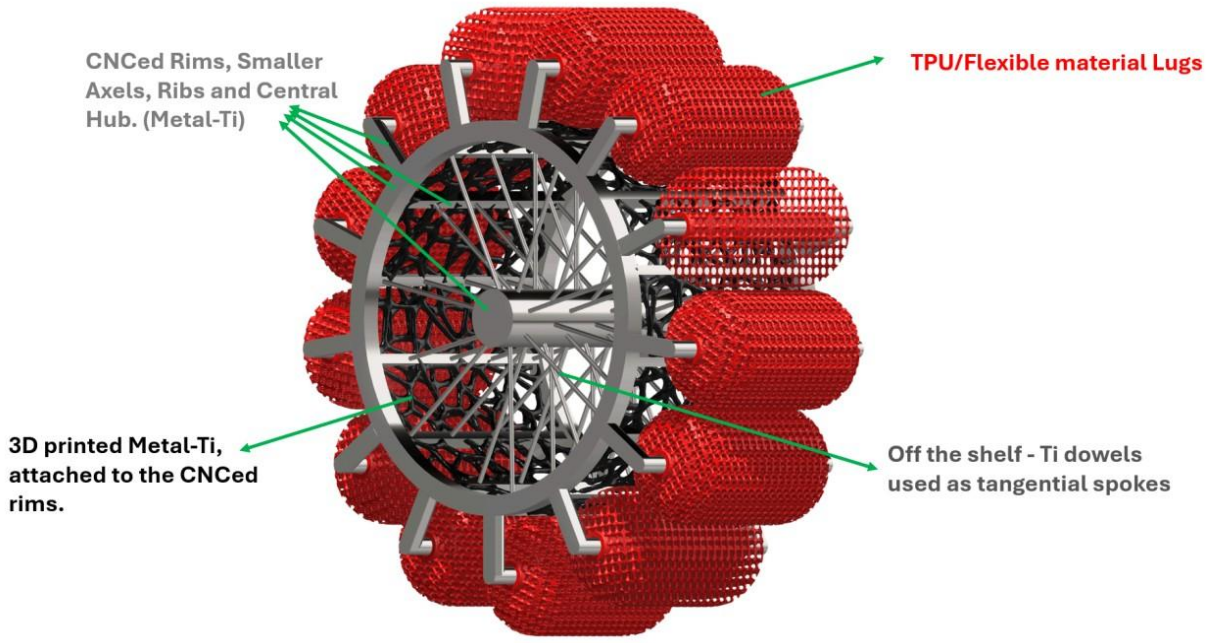

Figure 2: Hybrid-manufactured Mars rover wheel design

Based on the above-discussed customer needs and design constraints, the team came up with the wheel design shown above in Figure 2. This Figure depicts a hybrid-manufactured Mars rover wheel comprising CNC-machined titanium components, LPBF-fabricated internal lattice, and ME-printed TPU tread lugs. Design optimized for structural integrity and adaptability on Martian terrain. The details of this design and its components will be discussed in a later section.

III. AM Process Selection

A. AM Processes

The fabrication of the proposed Mars rover wheel leverages a hybrid manufacturing strategy that combines CNC machining and additive manufacturing (AM) to exploit the respective strengths of each process. This multi-process integration enables the realization of a lightweight, structurally optimized, and functionally graded wheel assembly suitable for operation in extreme extraterrestrial environments. For each manufacturing process, the justification for doing so is linked to the customer requirements and constraints.

The selected modalities are:

- **CNC machining for high-load metallic subcomponents**
- **Laser Powder Bed Fusion (LPBF) for the internal lattice of Ti-6Al-4V**
- **Material Extrusion (ME) for polymeric tread modules of TPU 75D with additives**

a. CNC Machining of Metallic Rim, Hub, and Structural Ribs:

CNC machining is utilized for fabricating the outer rims, central hub, and radial ribs, which serve as the high-load-bearing framework of the wheel. The selected material is Ti-6Al-4V, consistent with aerospace standards.

Justification for CNC Machining:

- CNC machining ensures high-precision geometries and tolerances ($< \pm 10$ μm), particularly critical at load interfaces such as axle sockets, dowel slots, and interlocking surfaces for modular integration [7].
- Unlike AM processes, subtractive machining avoids microstructural inhomogeneity or residual stress accumulation, resulting in isotropic mechanical properties ideal for torque transfer and fatigue-critical regions.
- Machined radial ribs provide structural reinforcement against radial deflection, while the central hub is designed to withstand torsional loads during rover traversal over uneven terrain.
- Titanium's low coefficient of thermal expansion and natural oxide passivation ensure operational stability across Martian thermal cycles and abrasive soil exposure [8].
- While material and tooling costs are high, with per-part machining costs ranging from $300–800 [9], depending on complexity, these components are limited in number and critical in function, justifying the investment.
- CNC machining is also critical for post-processing of LPBF components, especially in regions requiring high-fidelity mechanical interfaces or insertions.

b. Laser Powder Bed Fusion (LPBF) for Topology-Optimized Internal Lattice

The internal lattice structure, occupying the volume between the hub and the rim, is fabricated using LPBF, a high-resolution metal AM process compatible with Ti-6Al-4V.

Justification for LPBF:

- LPBF allows the realization of load-adaptive lattice geometries that cannot be machined using conventional methods. The structure is engineered for shock absorption, localized compliance, and stress redistribution.
- LPBF-fabricated Ti-6Al-4V parts, when HIPed (Hot Isostatic Pressed) and heat-treated, exhibit high tensile strengths with low mass penalty, enabling dynamic energy dissipation without failure [10].
- Lattice Customization: The lattice can be spatially graded to exhibit site-specific stiffness and damping properties, critical for reducing vibrational loads during traversal of rocky or granular terrain.
- Minimal Assembly Interfaces: LPBF consolidates complex geometries into monolithic components, eliminating fasteners and reducing failure-prone interfaces.
- LPBF is capital-intensive, and titanium powder feedstock contributes to higher per-part costs for lattice components. However, its material efficiency and the performance benefit it brings in critical structures make it suitable for low-volume, high-reliability builds, such as for space/extraterrestrial exploration usages.

c. Material Extrusion (ME) for Flexible Polymeric Tread Modules

The outer tread lugs, constructed from a high-durometer TPU (Thermoplastic Polyurethane), are fabricated using Material Extrusion (ME), commonly known as Fused Deposition Modeling (FDM).

Justification for ME:

- TPU offers high tear resistance, flexibility at sub-zero temperatures, and resistance to Martian dust abrasion, making it an ideal candidate for tread material [11].
- ME enables direct fabrication of lattice-based lugs with engineered porosity and grip-enhancing textures. The perforated structure promotes dust ejection and adaptability to granular regolith.
- ME allows for batch or on-demand production of tread units, which are modular and replaceable. This is ideal for mission scenarios involving robotic repair or human extravehicular activity (EVA). The simplicity of ME hardware further supports future adaptation for on-demand manufacturing in the field or extraterrestrial environments, including robotic in-situ repair.
- The polymer maintains mechanical performance in cryogenic environments, providing robust ground interaction over varied terrain.

d. Summary:

Table 2: Component-wise machining summary

Component	Material	Process	Cost Category	Notes
Rim, hub, ribs	Ti-6Al-4V	CNC Machining	Moderate to High	High precision, low-volume; essential for load-bearing skeleton
Internal lattice on rim	Ti-6Al-4V	LPBF (SLM)	High	Complex geometry; topology-optimized, monolithic shock damping
Outer tread modules/ Lugs	TPU (Shore 75D) with additives	ME	Low	Modular, easily replaceable, scalable

B. AM Machine Selection

The team used a decision selection matrix, shown in Table 3, in order to decide which AM machines would be most appropriate for fabricating the Mars rover wheel, based on the materials decided and discussed in the previous section. The wheel includes a titanium alloy lattice on the rim, which must be manufactured using LPBF, and 13 flexible polymeric tread modules, which must be manufactured using ME. These manufacturing requirements necessitate the use of two separate AM machines, which will be chosen and explained below.

Table 3a: ME Machine Decision Selection Matrix [12, 13]

Criteria	Weight	Ultimaker S5	Markforged FX20
Resolution	30%	3	4
Material Strength	40%	3	4
Build Volume	20%	3	4
Cost	5%	5	2
Post-process simplicity	5%	5	5
Total (weighted)		3.2	3.95

Table 3b: SLM Machine Decision Selection Matrix [14, 15]

Criteria	Weight	EOS M400	Renishaw AM 400
Resolution	35%	5	4
Material Strength	35%	5	4
Build Volume	15%	4	4
Cost	10%	3	3
Post-process simplicity	5%	2	2
Total (weighted)		4.5	3.95

The Ultimaker S5 was chosen for evaluation because of its relatively low cost compared to its capabilities, and its availability and familiarity as a result of being in some labs at Virginia Tech. The Markforged FX20 was chosen as an industrial powerhouse to evaluate the advantages of fully-funded industrial level production. SLM machines are not available at the consumer level, so both machines chosen for that comparison were selected for their resolution and reliability in industrial applications.

The weighting of the criteria in Table 3 was calculated using pairwise comparison tables for each AM process, shown in Table 4. The ranked customer needs from Table 2 were used to select the criteria for table Table 3 and Table 4. Durability is the highest ranked customer need, which will be heavily influenced by the finished material strength the AM machine is capable of producing, and by the resolution of the AM machine. Traction is the second-highest ranked customer need, which will be largely decided by material selection and part design, but will also be influenced by resolution. Adaptability and weight both ranked third in Table 2. Adaptability will be influenced mostly by design and material selection, but material strength and resolution will also influence this need. Weight will be influenced by both resolution and material strength, as both metrics will ensure that parts can be manufactured with minimal infill and wall thickness while maintaining strength. Manufacturability ranked fifth in customer needs, and it will be influenced by resolution, material strength, build volume, and post-processing simplicity to ensure the part can be accurately manufactured and that it will meet its durability requirements. Cost is also a factor to consider in manufacturability to ensure production of the part can be achieved financially, but it is much less important in this application than the previously mentioned criteria. Compatibility ranked sixth in customer needs and will mostly be fulfilled through design, but resolution also plays a small part in ensuring dimensions can be accurately manufactured to ensure compatibility with existing hardware. Finally, cost was ranked as the least important customer need with a relative weight of 0%, but it was included in the pairwise comparison as lower production costs without sacrificing quality is always beneficial.

Table 4a: Pairwise Comparison for ME Machine Criteria

	Resolution	Material Strength	Build Volume	Post-Processing	Cost	SUM	WEIGHT
Resolution	-	0	1	1	1	3	**30%**
Material Strength	1	-	1	1	1	4	**40%**

Build Volume	0	0	-	1	1	2	**20%**
Post-Processing	0	0	0	-	0.5	0.5	**5%**
Cost	0	0	0	0.5	-	0.5	**5%**

Table 4b: Pairwise Comparison for SLM Machine Criteria

	Resolution	**Material Strength**	**Build Volume**	**Post-Processing**	**Cost**	**SUM**	**WEIGHT**
Resolution	-	0.5	1	1	1	3.5	**35%**
Material Strength	0.5	-	1	1	1	3.5	**35%**
Build Volume	0	0	-	0.5	1	1.5	**15%**
Post-Processing	0	0	0.5	-	0.5	1	**10%**
Cost	0	0	0	0.5	-	0.5	**5%**

The Markforged FX20 outperforms the UltiMaker S5 in resolution, material strength, and build volume, with an even score in post-process simplicity, and a much lower score in cost. The Markforged FX20's higher scores in resolution, strength, and build volume were expected from a comparison between an industrial-grade printer and a high-end hobbyist printer. The Markforged FX20 is the better choice for large-scale production, especially when outsourcing manufacturing to a facility that operates multiple machines at high utilization, but the UltiMaker S5 would be better for prototyping and testing.

The EOS M400 and Renishaw AM 400 both scored the same in build volume, cost, and post-processing simplicity, but the EOS M400 outperformed the Renishaw machine in resolution and material strength. These scores were expected as the EOS M400 is usually 20-30% more expensive and has been an industry standard machine for close to a decade.

Candidate Machines

Table 5: AM Machine Details

Machine	**Process**	**Material**	**Notes**
UltiMaker S5	ME	PLA/TPU	Affordable, ideal for iterative prototyping
Markforged FX20	ME	PLA/TPU, Continuous Fiber Composites	Industrial-grade ME machine; supports high-strength parts with carbon fiber reinforcement; suitable for functional prototyping and low-volume production
EOS M400	SLM	Ti-6Al-4V	High-resolution, industry standard
Renishaw AM 400	SLM	Ti-6Al-4V	Good precision, moderate cost

Reflections & Recommendations

- **EOS M400** is the best choice for the final production of the titanium parts with high fidelity and material capability.
- **UltiMaker S5** suits early design phases with flexible TPU. But **Markforged FX20** is a better option for final, large-scale production.
- The choices align well with functional and manufacturing goals.

Final Recommendation: EOS M400 **(Ti-6Al-4V)** ; UltiMaker S5 (for prototyping) and Markforged FX20 (for final production) **(TPU)**

NOTE: *While the selected ME machines (UltiMaker S5 and Markforged FX20) effectively support prototyping and production with conventional TPU materials, compatibility with advanced TPU formulations, such as TPU 75D blended with UV-resistant additives, needs further evaluation. The Mars environment presents unique challenges, including extreme temperature variations, UV radiation, and abrasive regolith, which necessitate using specialized polymers with enhanced thermal stability, abrasion resistance, and radiation durability. Currently, the Markforged FX20, with its higher temperature capabilities and reinforced printing capability, may support printing of advanced TPU blends with appropriate tuning. However, validation tests and possibly minor hardware modifications might be necessary to achieve optimal print quality and reliability with TPU 75D and UV additives. Therefore, preliminary trials and further material-machine compatibility studies are strongly recommended before proceeding with full-scale manufacturing for Martian surface applications.*

IV. DfAM (Design for Additive Manufacturing) Conceptual Design and Selection

A. Wheel Design Concepts

To identify the most effective design solution for a modular, high-performance Mars rover wheel, a variety of design concepts were explored. These concepts incorporate distinct Design for Additive Manufacturing (DfAM) heuristics, each targeting specific customer needs such as adaptability, repairability, lightweighting, and manufacturability. The four most promising concepts are presented below, culminating in a final candidate that directly informed the detailed design phase. Each image presented below was first hand-drawn during the brainstorming phase and then brought to life using AI prompts for ease of understanding by the reader, and as a good way of presenting the ideas.

a. Concept A:

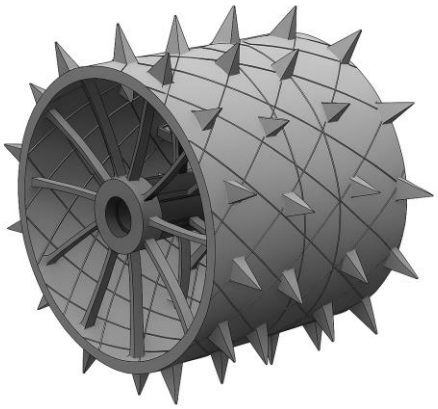

Figure 3: Spiked cylindrical shelled wheel with a central hub and thick spokes

As shown in Figure 3, concept A is a rigid, cylindrical outer shell with integrated pyramidal spikes oriented radially outward for improved traction in loose Martian regolith. The internal core is designed as a solid wall for passive stiffness. It also has treads over the surface for added traction.

DfAM Heuristics: The shell and spikes are fabricated as a monolithic unit, eliminating fasteners or joints; Spike orientation and shell curvature are designed to minimize overhangs in AM; Having a lattice shell can enable light-weighting while maintaining structural shell continuity.

Customer Needs Addressed: Traction, dust mitigation, manufacturability, and impact survivability.

Limitations: The rigid nature of this design reduces terrain adaptability and shock compliance. No modularity means field replacement of damaged spikes or deformation zones is infeasible.

b. Concept B:

Figure 4: Spring-spoked wheel with hex cladding in fabric structure on outer surface

As shown in Figure 4, concept B is a deformable wheel composed of long, flexible spring spokes radiating from a central hub, supporting a mesh-like outer skin inspired by NASA's Superelastic Tire concept. This allows for terrain conformity without internal inflation.

DfAM Heuristics: Replaces mechanical suspensions with springy additively manufactured spokes; Designed as a continuous or layered mesh, printable in flexible metal or polymer; Inner geometry maximized for deflection under load with material minimization.

Customer Needs Addressed: Adaptability, passive shock absorption, modularity (via replaceable spring bundles).

Limitations: Difficult to control sidewall deflection; more complex to assemble; less traction control unless additional tread pattern is applied or bonded. Fabric can also rupture.

c. Concept C:

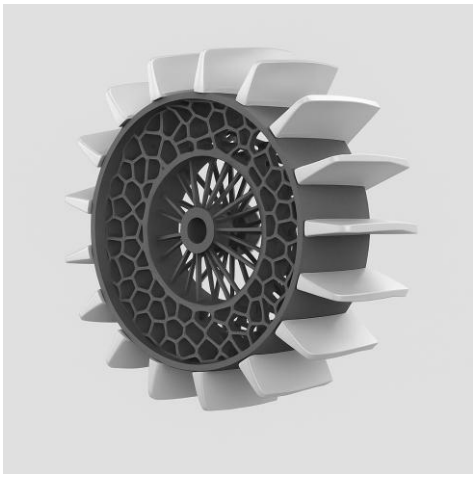

Figure 5: 2D lattice inner core wheel with flat horizontal paddle structures

As shown in Figure 5, concept C is a monolithic or semi-monolithic structure built around a 2D solid lattice (can be Voronoi or gyroid), over which modular paddle-like lugs are mounted. Each lug is positioned at an angle to promote forward movement through loose terrain.

DfAM Heuristics: The internal core is topologically optimized for weight and stress distribution; Only manufacturable through high-resolution AM; Paddles can be switched to allow terrain-specific tuning or swapping.

Customer Needs Addressed: Traction, redundancy, terrain adaptability, structural compliance.

Limitations: Increased lug complexity (rotation systems or axles); less straightforward AM compatibility at full scale without multi material deposition. Too long paddles can make motion difficult and can break under extra loads.

d. Concept D:

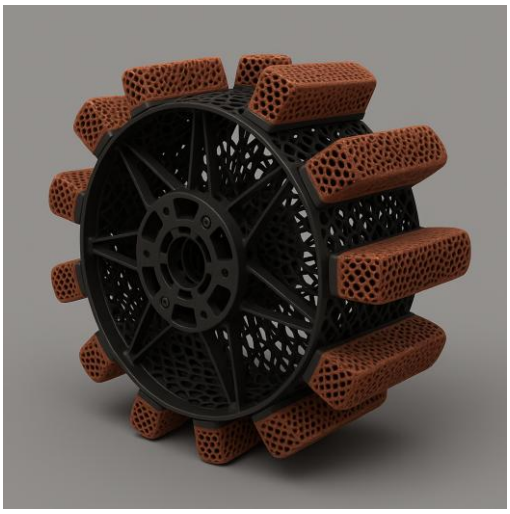

Figure 6: Cuboidal- lattice modular paddle wheel with hybrid lattice and spoked core

As shown in Figure 6, concept D is a structurally optimized wheel with a central metallic lattice (LPBF or truss-printed) and modular cuboidal TPU tread elements radially mounted to the outer rim. The lugs are mounted horizontally, perpendicular to the wheel's axis, close to the surface for optimal ground contact and compact packaging.

DfAM Heuristics: Central core is printed with mechanical grading for impact energy absorption; Lightweight because of the lattice-based design; TPU tread elements manufactured via ME/FDM; Ti skeleton via LPBF and CNC; Cuboidal tread pods are reprintable and attach to socketed or slotted arms for easy in-field replacement.

Customer Needs Addressed: Durability, adaptability, modularity, manufacturability (both Earth-based and in-situ), and weight reduction.

After systematically evaluating all conceptual designs against customer needs and engineering specifications, the modular cuboidal-lug wheel (Concept D) emerged as the most suitable option for further development. This selection is strongly supported by the outcomes of the Quality Function Deployment (QFD) analysis, where durability (28.57%), traction (19.05%), and adaptability and weight (16.67%) were identified as the most critical needs for Martian rover performance. Concept D directly addresses these top-ranked priorities through its topology-optimized titanium lattice core, which minimizes weight while providing high mechanical strength and fatigue resistance. Its radially mounted TPU tread modules, each incorporating porous lattice structures, allow for localized deformation, effective shock absorption, and consistent terrain contact, ensuring reliable movement over loose regolith, rocky slopes, and variable inclines.

In terms of manufacturability, which also scored highly in the QFD, Concept D is fully aligned with DfAM heuristics. All components are designed to be produced via established additive processes: LPBF for the metallic core and hub, and ME for the flexible TPU treads. This not only supports rapid prototyping during development but also future in-situ fabrication on Mars, a key consideration for long-duration missions. The design also addresses repairability and low-cost maintenance by enabling easy detachment and replacement of individual tread lugs, avoiding the need for full wheel replacement in the field.

Furthermore, the wheel's central hub and dowel-based mounting interfaces are dimensioned for compatibility with existing rocker-bogie suspension systems, simplifying mechanical integration. This interoperability enhances the design's feasibility for current and next-generation rover architectures. Compared to more rigid or complex alternatives like Concept A, B, or C, Concept D provides a well-balanced solution that combines structural performance, lightweight efficiency, modular repairability, and additive manufacturability. These strengths, corroborated by QFD weighting and tied to mission-specific needs, make Concept D the most viable, scalable, and operationally resilient concept for Martian surface mobility. The details of the final design, as already shown in Figure 2, will be discussed in the next section.

B. Lug Design Concepts

Selecting the optimal lattice topology for TPU 75D tire lugs requires balancing mechanical performance with practical functionality in the abrasive, dusty environment of Mars. Cellular architectures can be tailored to deliver specific stiffness, strength, and energy-absorption characteristics, but their void geometry also dictates how easily regolith can escape under cyclic loading. In this study, we benchmark four candidate lattices—Hex-Vase, Octa-Hedroid, Dodeca-Hedron, and Quad-Diametral—under identical compressive loads and support conditions. Each paragraph below describes the unique features, expected performance, and practical considerations of one topology.

a. **Hex-Vase Lattice**

The Hex-Vase lattice combines vertical, honeycomb-inspired ribs with gentle "vase"-like curvature at each node, producing a predominantly uniaxial stiffness along the loading direction. Its six-fold symmetry yields high in-plane rigidity, making it an efficient energy absorber under compressive loads. However, the thin membranes connecting the hexagonal struts introduce anisotropy: off-axis loading tends to concentrate stress at the membrane junctions, increasing risk of local yielding. Moreover, the relatively narrow, planar

voids between ribs offer limited self-cleaning; regolith particles can become wedged, reducing effective contact area and traction over time.

b. **Octa-Hedroid Lattice**

Rooted in the geometry of the Platonic octahedron, the Octa-Hedroid lattice interconnects struts at virtual octahedral vertices to create a near-isotropic network.Its well-balanced connectivity makes it a proven choice in lightweight structural applications [16]. Its moderate void fraction and uniform node connectivity deliver balanced stiffness and strength in all directions, with peak von Mises stresses around 15 MPa and deflections under 0.6 mm in bench-scale tests. The open, interconnected triangular channels excel at shedding trapped soil and small pebbles under vibration, providing a self-cleaning advantage critical for maintaining traction on dusty terrain. When scaled to full-size tire lugs, increasing the strut diameter can recover additional stiffness without sacrificing these large egress pathways.

c. **Dodeca-Hedron Lattice**

By linking struts at the corners of virtual dodecahedra, this topology maximizes internal volume while maintaining a lightweight skeleton. The high void fraction offers superior damping and compliance—ideal for smoothing out uneven terrain—but inherently reduces bulk stiffness. Under equivalent loads, this lattice deflects more than its counterparts, and its lower node connectivity can lead to localized bending at strut intersections. Although debris clearance is excellent due to large spherical voids, the risk of excessive deformation and fatigue under full-scale rover loads may limit its long-term durability without significant strut thickening.

d. **Quad-Diametral Lattice**

Composed of interlocking square-based diamond units, the Quad-Diametral lattice provides directional stiffness along two orthogonal axes. Its four-strut nodes create a robust network capable of resisting moderate loads, but the narrow, tortuous channels between cells tend to trap fines and small rocks. Bench-scale FEA revealed high peak stresses (>200 MPa) in localized regions, indicating stress concentration and potential for premature yielding. While printability in TPU is straightforward due to simple strut geometry, the impractical void architecture undermines both self-cleaning and fatigue life under cyclic loading.

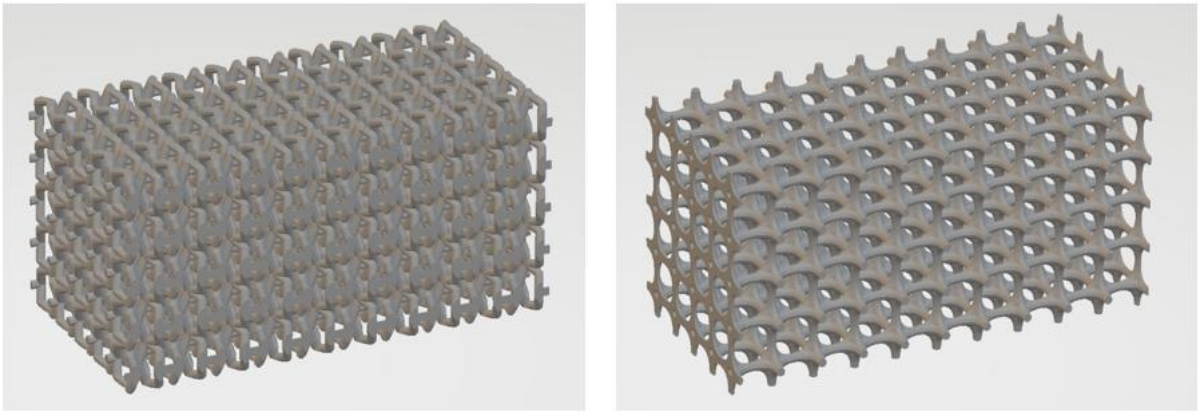

(a) (b)

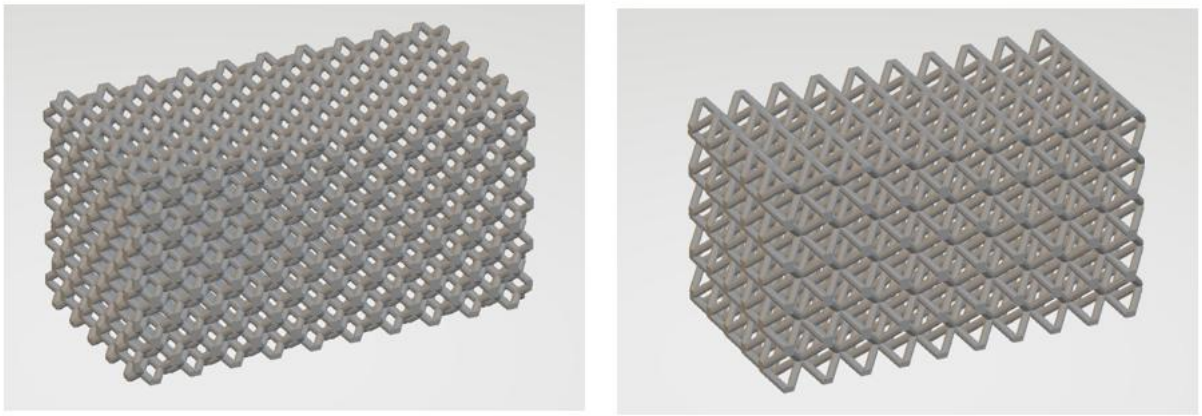

Figure 7: 4 candidate lattice structures.
(a) Hex-Vase Lattice (b) Octa-Hedroid lattice(c) Dodeca-Hedron Lattice(d) Quad-Diametral Lattice

Among the four lattices, the Octa-Hedroid topology emerges as the most balanced solution for Martian tire lugs as depicted in the Engineering Analysis Section. It combines near-isotropic stiffness, moderate stress levels, and large interconnected voids that facilitate debris egress—features that no other candidate simultaneously offers. By scaling up the strut diameter in full-scale tire designs, engineers can further enhance stiffness to meet rover-weight requirements while preserving the essential self-cleaning channels. This synergy of mechanics and functionality makes the Octa-Hedroid lattice the recommended architecture for future TPU 75D tire-lug prototypes.

V. Embodiment and Detail Design

A. Final Design

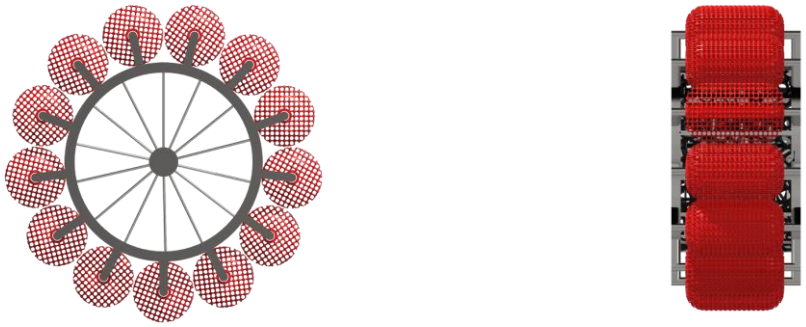

Figure 8: (a) Front view of the CAD model; (b) Side view of the CAD model.

The final design developed for the Mars rover wheel represents a carefully engineered solution that balances terrain adaptability, structural durability, and manufacturability through a hybrid approach of additive and subtractive manufacturing. This design is the outcome of iterative conceptual design processes informed by performance-driven thinking, Design for Additive Manufacturing (DfAM) principles, and customer needs evaluated via a Quality Function Deployment (QFD) framework. This final design was derived from concept D discussed earlier.

Figure 7 represents the front and side views of the hybrid-manufactured Mars rover wheel comprising CNC-machined titanium components, LPBF-fabricated internal lattice, and ME-printed TPU tread lugs. Figure 2 represents the isometric view of the same. The configuration features the following subsystems:

- **CNC-Machined Titanium Skeleton**:

The titanium skeleton forms the foundational structure of the wheel, consisting of outer rims, a central hub, and radial reinforcing ribs and spokes. These components are machined from Ti-6Al-4V using CNC techniques due to the need for precision in dimensional tolerances and surface finish—especially at critical mating interfaces such as the hub and rim. Titanium's aerospace-grade mechanical reliability ensures the structural frame can handle dynamic loading during rough terrain traversal. CNC was specifically chosen here to avoid the microstructural inconsistency and tolerance limitations often associated with additive manufacturing for complex mechanical interfaces.

- **LPBF-Printed Titanium Lattice Core**:

Positioned between the hub and along the rim surface, the internal lattice structure serves as a compliant layer to distribute and absorb radial and torsional loads. Siemens NX computational topology optimization tools were used to help develop the lattice structure. This strategy allowed us to reduce material usage without compromising functional integrity. The LPBF process is ideal here as it enables intricate lattice geometries to be fabricated with minimal supports and high resolution, reducing both weight and material cost while retaining shock resistance.

- **Titanium Tangential Dowels**:

Tangentially arranged titanium dowels serve as spokes that transfer torque from the central hub to the rim while maintaining alignment. Their orientation mimics that of a bicycle wheel, efficiently managing both compression and tension during rover maneuvers. These dowels are modular and replaceable, providing redundancy in the event of single-point failures. Although integral spoke configurations were considered, the simplicity and flexibility of dowel-based construction—especially for field repairs or scaling—led to its selection. The approach allows the use of standardized, off-the-shelf components for rapid prototyping and in-situ maintenance.

- **Modular TPU Lattice Tread Lugs**:

The tread lugs interface directly with the Martian terrain, and their role is to provide traction, dust clearance, and compliance with uneven surfaces. Each lug is fabricated using FDM-compatible TPU 75D with additives, selected for its tear resistance and performance at low temperatures along with UV resistance. A custom octahedral lattice structure within each lug, designed with high porosity, enables controlled deformation and impact absorption. Lattice parameters were derived from established DfAM guidelines and manual tuning using NX Siemens. The modularity of the lugs means they can be printed and replaced individually, including on Mars using portable extrusion-based AM systems, thus reducing launch mass and extending operational life.

Together, these subsystems form a functionally partitioned, structurally interdependent design that supports the full mission context from launch to terrain traversal to potential post-deployment repair. Now, let us take a look at the two main components of this design in further detail. The Titanium part and the TPU part.

a. Titanium Structure

Figure 9: (a) Front view of the titanium components; (b) Side view of the titanium components

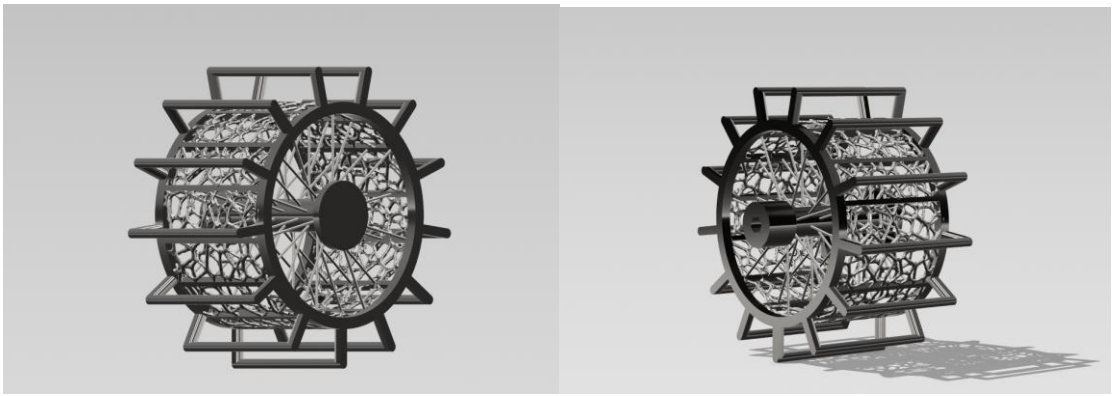

Figure 10: (a) Isometric view of the Titanium components (anterior); (b) Isometric view of the Titanium components (posterior)

b. TPU Structure

Figure 11: (a) Front view of a singular TPU component; (b) Side view of a singular TPU component

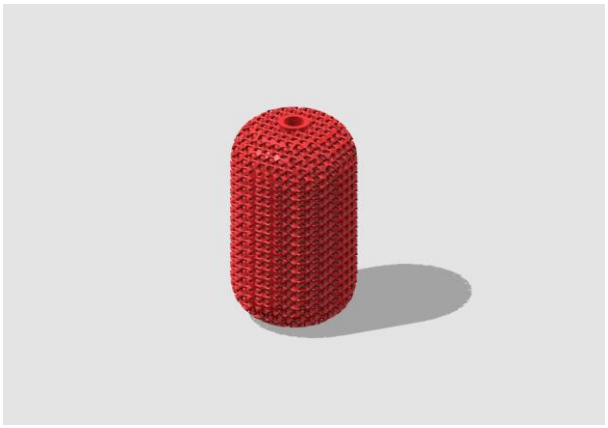

Figure 12: Isometric view of a singular TPU component (anterior)

c. Dimensions of the Design

As shown in Figure 12, the drawing depicts all the dimensions of the various components of the design. It is important to note that only a single lug has been shown here as a simplified version to keep the drawing clean and easy to understand. These drawing dimensions conform to the prototype design and are easily scalable for manufacturing the scaled version for real-life deployment, depending on the requirements, may it be for a rover or for an extra-terrestrial human vehicle. All dimensions here are in mm.

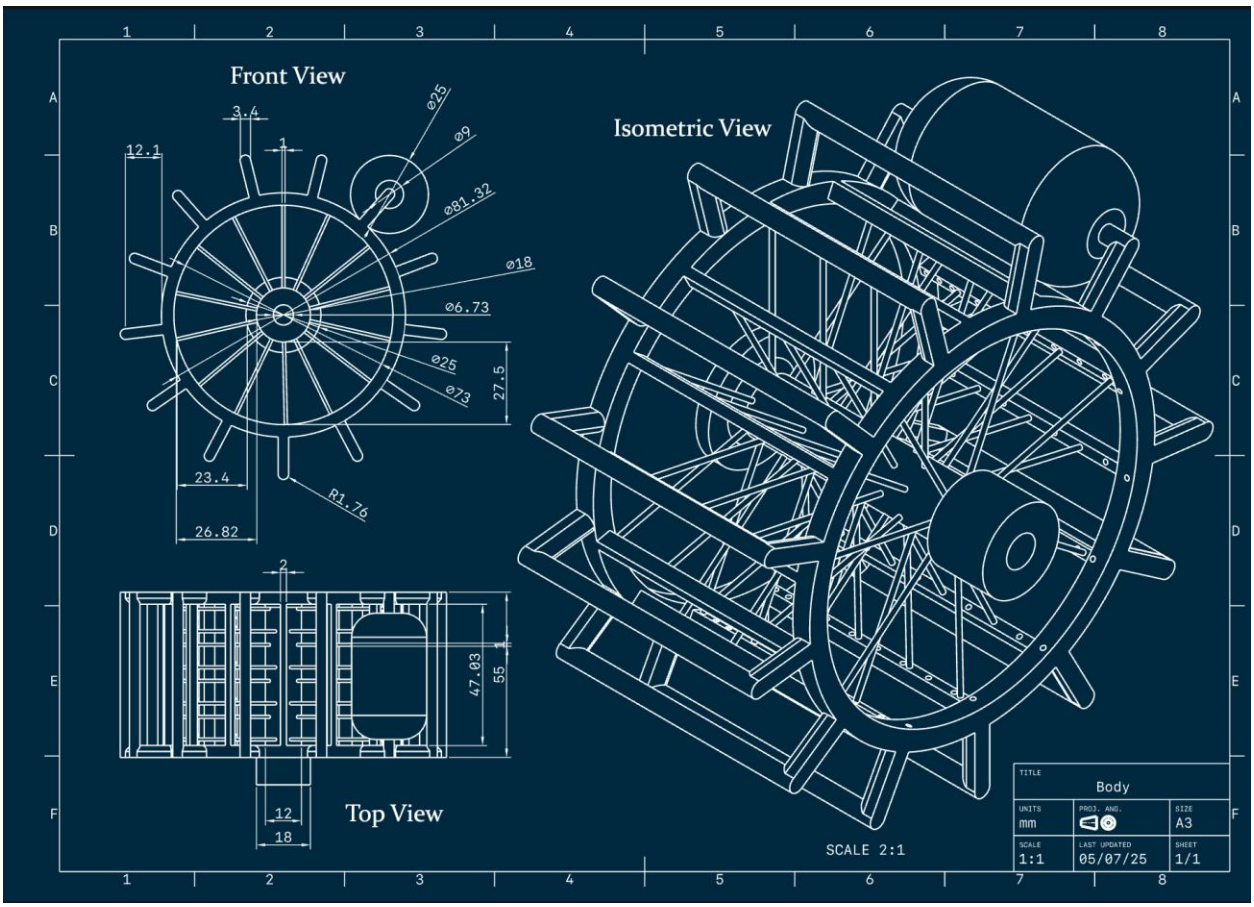

Figure 13: CAD drawing of the design generated, showing all the component dimensions

VI. Design Analysis

A. Design Analyses

In the development of next-generation tire lug-inserts for extraterrestrial rovers, selecting an optimal internal lattice topology is critical to balancing load-bearing capacity, energy absorption, and material efficiency. Additive manufacturing of elastomeric lattices—such as those fabricated from TPU 75D—enables the creation of complex cellular architectures that can be tailored to specific mechanical requirements. However, the vast design space of possible lattice geometries demands a systematic benchmarking approach to identify which structure best meets the competing demands of stiffness, strength, and manufacturability.

To this end, we conducted a finite-element study on four candidate lattices—Hex-Vase, Octa-Hedroid, Dodeca-Hedron, and Quad-Diametral—subjected to a uniform compressive load with a factor of safety of 1.1. By comparing maximum deflection, peak stress, and stress distribution under identical boundary conditions, we aim to establish a clear performance hierarchy among these topologies. This benchmarking exercise provides quantitative guidance for selecting the most promising lattice design, ensuring that final tire-lug prototypes will deliver reliable traction, minimal deformation, and long-term durability in the demanding Martian environment.

Table 6: Summary table of material properties for TPU 75D [17]

Property	Symbol	Typical Value	Units
Density	ρ	1.21	g/cm³
Young's modulus (tensile)	E	30	MPa
Poisson's ratio	ν	0.40	—
Tensile strength (ultimate)	σ	25.5	MPa

LATTICE MODEL SETUP:

The finite-element analysis (as depicted in Figure 14) was performed on a cubic block (100mm x 50mm x 50mm) of repeating lattice cells fabricated from TPU 75D, with a factor of safety (FOS) of 1.1 applied to the material properties (Actual values (No FOS) depicted in Figure 7). A uniform vertical load was imposed across the entire top face of each lattice specimen, while all degrees of freedom were rigidly fixed at the bottom face to simulate a fully supported tire lug. This boundary condition replicates the worst-case compressive loading scenario that a Martian tire lug would experience when bearing the vehicle's weight on uneven terrain.

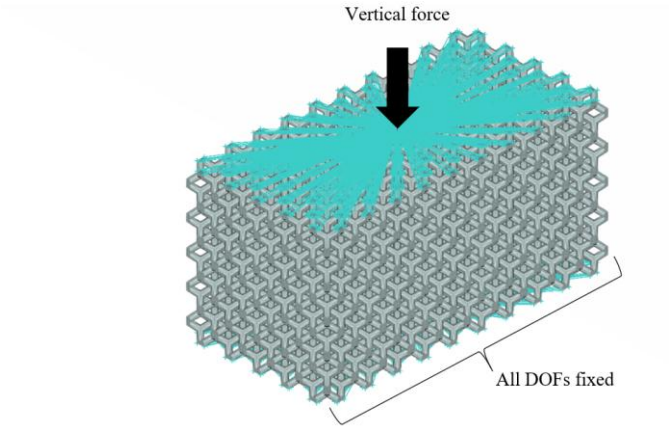

Figure 14: Finite Element Analysis Model Setup

Four distinct lattice geometries (as depicted in Figures 15 and 16)—Hex-Vase, Octa-Hedroid, Dodeca-Hedron, and Quad-Diametral—were each subjected to the same loading and support conditions. Among these, the Octa-Hedroid lattice exhibited the smallest maximum vertical deflection (0.57 mm) and a moderate peak von Mises stress of 15 MPa. By contrast, the Hex-Vase and Dodeca-Hedron lattices deflected by 0.75 mm and 0.72 mm, respectively, with stresses of 44 MPa and 9 MPa; while the Quad-Diametral lattice showed excessive deflection (1.40 mm) and extremely high stress concentrations (217 MPa), indicating poor suitability for repeated cyclic loading.

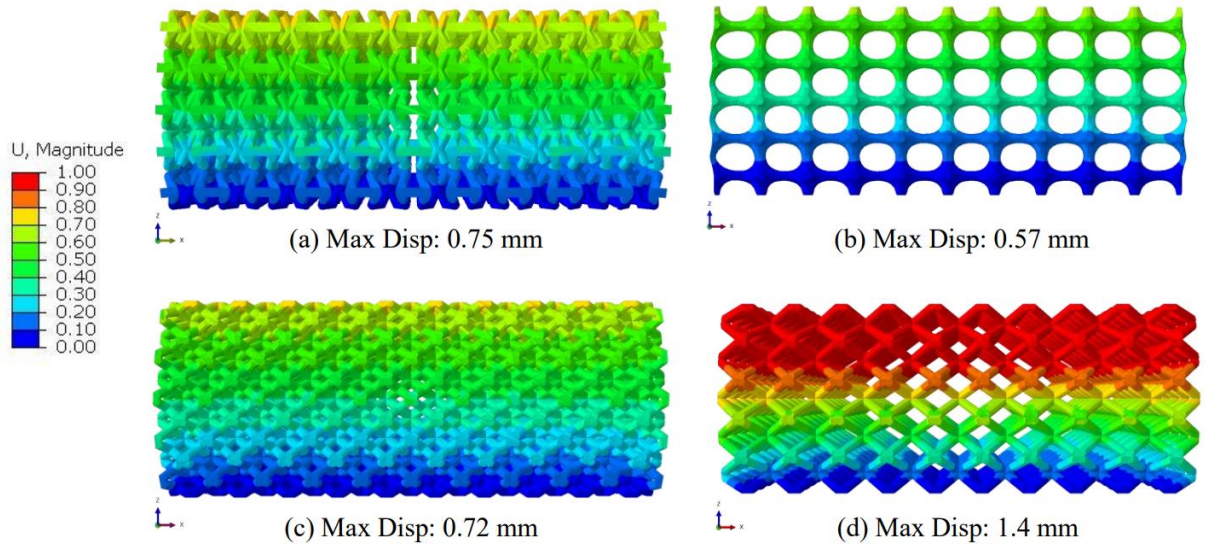

Figure 15: Deformation Plots for the 4 candidate lattice structures.

(a) Hex-Vase Lattice (b) Octa-Hedroid lattice(c) Dodeca-Hedron Lattice(d) Quad-Diametral Lattice

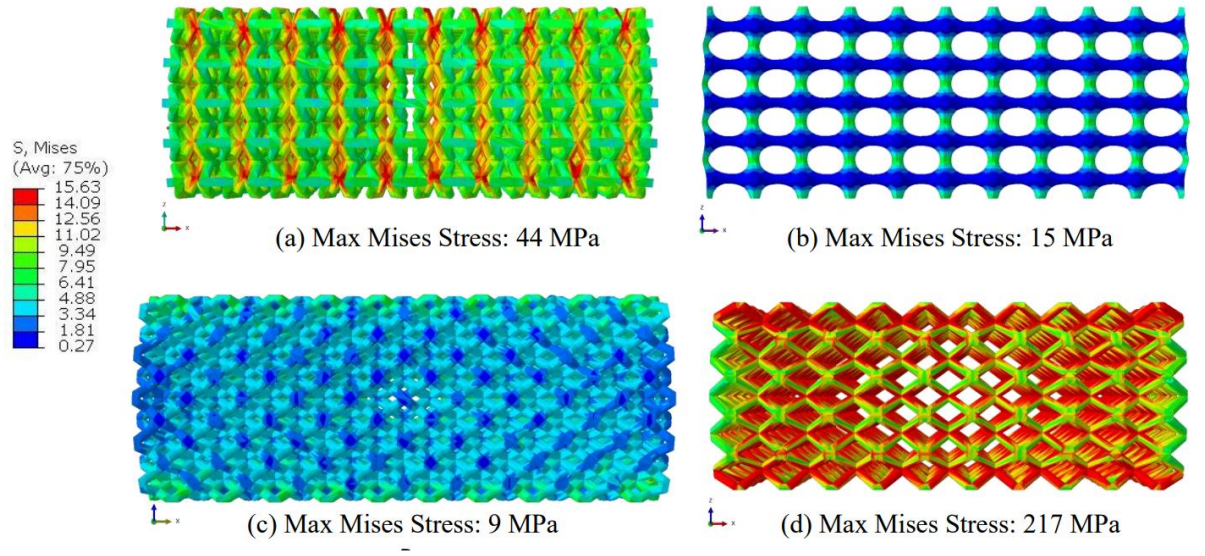

Figure 16: Von-Mises Stress Plots for the 4 candidate lattice structures.

(a) Hex-Vase Lattice (b) Octa-Hedroid lattice(c) Dodeca-Hedron Lattice(d) Quad-Diametral Lattice

From a stiffness perspective, the Octa-Hedroid's low deflection under load translates to a higher effective modulus, which helps maintain lug geometry and tire-ground contact area during operation. Its peak stress of 15 MPa

remains well below the TPU 75D material's allowable stress (17.2 MPa), offering a comfortable safety margin against yielding or fatigue failure over many load cycles. Moreover, the stress distribution in the Octa-Hedroid lattice is relatively uniform, minimizing localized overstressing and potential crack initiation sites.

Beyond mechanical performance, the Octa-Hedroid topology strikes an excellent balance between structural complexity and printability (as depicted in Figure 22). Its network of interconnected struts avoids the pronounced overhangs seen in more intricate lattices, facilitating reliable additive manufacturing in rubber-like TPU without excessive support material or post-processing. This ensures consistent part quality and dimensional accuracy—critical factors for prototype tire lugs destined for the harsh Martian environment.

Table 7: Lattice Topologies Evaluations (Displacements are normalized to the same applied load)

Option	Topology	Max Disp. (mm)	Max von Mises Stress (MPa)
(a)	Hex-Vase	0.75	44
(b)	**Octa-Hedroid**	**0.57**	**15**
(c)	Dodeca-Hedron	0.72	9
(d)	Quad-Diametral	1.40	217

In summary, the Octa-Hedroid lattice offers the optimal combination of high stiffness, low stress, uniform deformation, and manufacturability for Mars tire lug applications. Its performance under simulated Martian loading conditions makes it the recommended topology for all future TPU 75D tire-lug designs, promising improved durability, load-bearing capacity, and traction consistency. Beyond its superior stiffness and low stress under load, the Octa-Hedroid lattice offers an extra practical benefit: its large, interconnected voids facilitate the egress of trapped Martian soil and pebbles. When implemented at full tire scale (with thicker struts for higher loads), these channels act as self-cleaning passages. Other candidate lattices—with tighter or more tortuous cell openings—would tend to accumulate debris, leading to progressive clogging and loss of traction. Thus, the Octa-Hedroid topology not only meets the mechanical requirements but also enhances operational reliability in a dusty, abrasive environment

To determine the optimal Octa-Hedroid lattice geometry for Martian tire lugs, we benchmarked two strut-diameter variants—0.40 mm and 0.60 mm—under identical compressive loading and support conditions. This comparison evaluates not only pure mechanical metrics (stiffness and stress) but also the practical requirement of self-cleaning, since trapped regolith can severely degrade traction over time.

Table 8: Comparative Lattice Topologies Evaluations (2 Octa-Hedroid lattice structures with different rod diameters)

Option	Rod Diameter	Max Disp. (mm)	Max von Mises Stress (MPa)	Relative Void Size	Debris Egress	Effective Stiffness
1	0.40 mm	0.57	15	Larger	Excellent	Moderate
2	0.60 mm	0.40	9	Smaller	Poor	High

In a head-to-head comparison (as depicted in Figure 17), the 0.60 mm-rod lattice unsurprisingly delivers higher stiffness (0.40 mm maximum deflection) and a lower peak von Mises stress (11.3 MPa) in our bench-scale tests. However, its tighter cell openings are prone to trapping Martian soil and pebbles, risking progressive clogging and loss of surface contact. Conversely, the 0.40 mm-rod lattice is slightly more compliant (0.57 mm deflection) and operates at a moderate peak stress of 15 MPa—still well below TPU 75D's design limit—while its substantially larger, interconnected voids facilitate debris egress under vibration. When scaling to a full-size tire lug, we can preserve this self-cleaning advantage by proportionally increasing the strut diameter, thereby restoring the required stiffness for rover-weight loads without sacrificing the lattice's natural debris-egress capability.

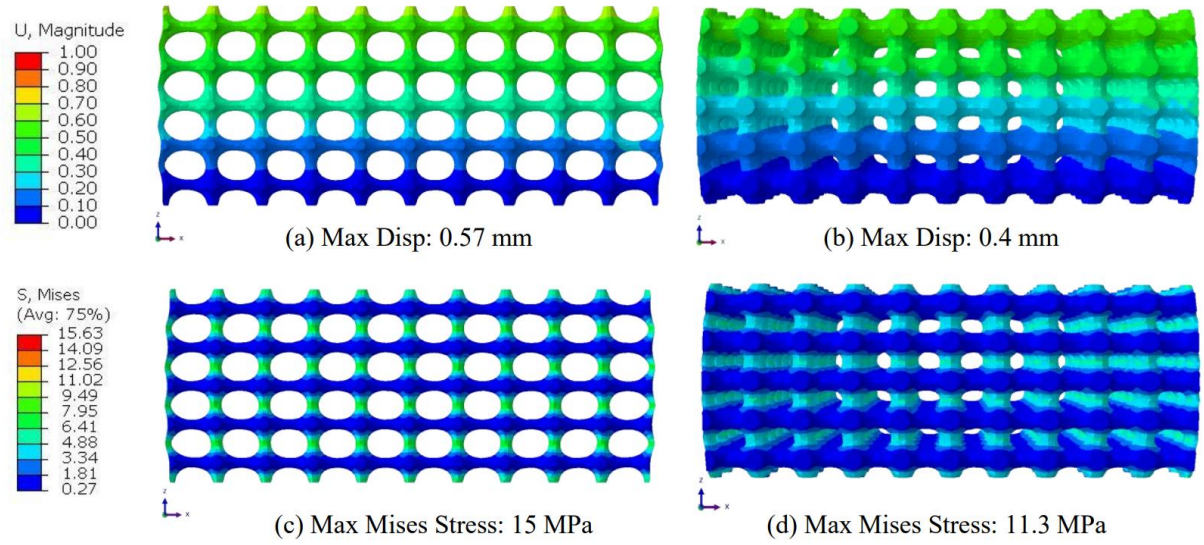

Figure 17: Deformation Plots for the 2 Octa-Hedroid lattice structures with different rod diameters.

(a) 0.4 mm (b) 0.6mm

Von-Mises Stress Plots for the 2 Octa-Hedroid lattice structures with different rod diameters.

(c) 0.4 mm (d) 0.6mm

VII. Prototyping

A. Printing Results

To validate the manufacturability and geometric fidelity of the final wheel design, a series of scaled and full-size prototypes were fabricated using additive manufacturing. These printing trials provided critical insight into feature resolution, structural behavior, and design-for-printability constraints, especially concerning the modular TPU lugs and intricate lattice elements.

a. Prototyping Setup and Materials

All components were printed in-house using a Bambu Lab P1S 3D printer, which was available to the team through a teammate's personal setup (Figure 18). This printer offers high-speed fused deposition modeling (FDM) with multi-material capability, making it suitable for iterative design validation under limited lab access conditions. The following materials were used:

- **PLA (Polylactic Acid)** for structural validation of the rim, hub, and lattice cores. (All Ti parts). Printed at 0.2mm layer thickness.
- **TPU 90A (Thermoplastic Polyurethane)** for flexible tread lug components to approximate compliant behavior. Printed at 0.16 layer thickness.

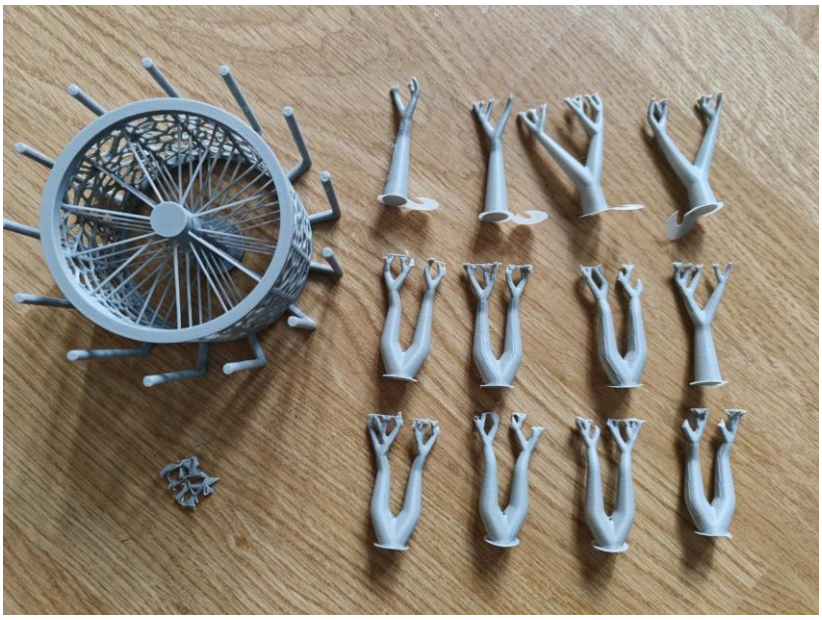

Figure 18: PLA parts printed in grey color, depicting the Ti components (the structures on right are the organic tree support structures used for printing the main component)

While the final mission-intended material is TPU 75D, the selected 90A variant allowed for prototyping with higher flexibility and greater tolerance to surface imperfections at the desktop scale.

Figure 19: (a) Front view of the prototype wheel system; (b) Side view of the prototype wheel system

Figure 20: Isometric view of the prototype wheel system (Grey = PLA; Red = TPU; Silver = Stainless Steel rod)

After printing all the components, they were assembled together and the prototype was fabricated as seen in Figures 19 and 20. 2 sets of prototypes were fabricated and each was connected using a Stainless Steel rod, which acts like an axle shaft.

B. Print Scaling and Resolution

Two sets of prints were produced:

- **1:2 scale prints** for early-stage geometry validation and assembly feasibility. (Figure 21, left)
- **1:1 scale prints** matching the actual dimensions of the final design for full validation of fit, function, and structural performance. (Figure 21, right)

The **1:2 scale** TPU lugs experienced early failure and delamination during handling and testing, especially at interfacial lattice regions. This behavior highlighted the fragility of small cross-sections in flexible materials and informed later iterations where wall thickness, infill density, and joint profiles were adjusted for improved robustness.

The **1:1 scale** prints, though more material-intensive and time-consuming, offered higher stability and a more realistic representation of the design. The larger-scale lattice structures are printed cleanly in PLA, with clear resolution of key features like interlocking sockets and dowel interfaces. In addition to that, for the lugs, it was noticed that increasing the scaling increased the structural integrity of the lugs' lattice structure and were able to take much

higher loads. Because of cost and time constraints, only a single lug was printed at 1:1 scale as seen in the Figure. Additionally, the spokes were not printed because of support structure constraints, and as this scale print was only for a physical representation, and did not play a physical/technical importance.

Figure 21: Left: 1:2 Scale prototype wheel system (Grey = PLA; Red = TPU); Right: 1:1 Scale prototype wheel system (Grey = PLA; Neon Yellow = TPU)

*C. **Manufacturability Observations***

Despite design efforts to minimize overhangs and support requirements, several manufacturability challenges were observed:

- TPU lugs required very slow print speeds (40–70 mm/s) to avoid stringing and maintain print adhesion. The one printed at full scale in neon yellow was printed at a higher speed (~ 100mm/s), and stringing was noticed. (Figure 22, Left) Hence, if these parameters are optimized, it is noticed that with an increase in scale, the print keeps getting better!
- Thin-walled lattice features in both PLA and TPU suffered from minor warping or sagging in unsupported zones, emphasizing the need for careful orientation and use of support structures during slicing. (Figure 22, Right)
- The cylindrical lugs, in particular for the 1:2 scale resolution, showed increased print failure rates due to their unsupported edges and complex internal geometry. This led to adjustments in orientation, shell thickness and print nozzle size to improve success rates.
- Layer adhesion in TPU, especially at lug-wall intersections, was a critical failure point — suggesting the need for increased wall count or possibly switching to a harder TPU (like 75D) with optimized cooling in future tests.

The **central hub** and **dowel sockets** printed cleanly in PLA at both scales, validating their tolerances and rotational fit. These components did not require post-processing and matched their CAD counterparts within ±0.5 mm — acceptable for functional validation at this stage.

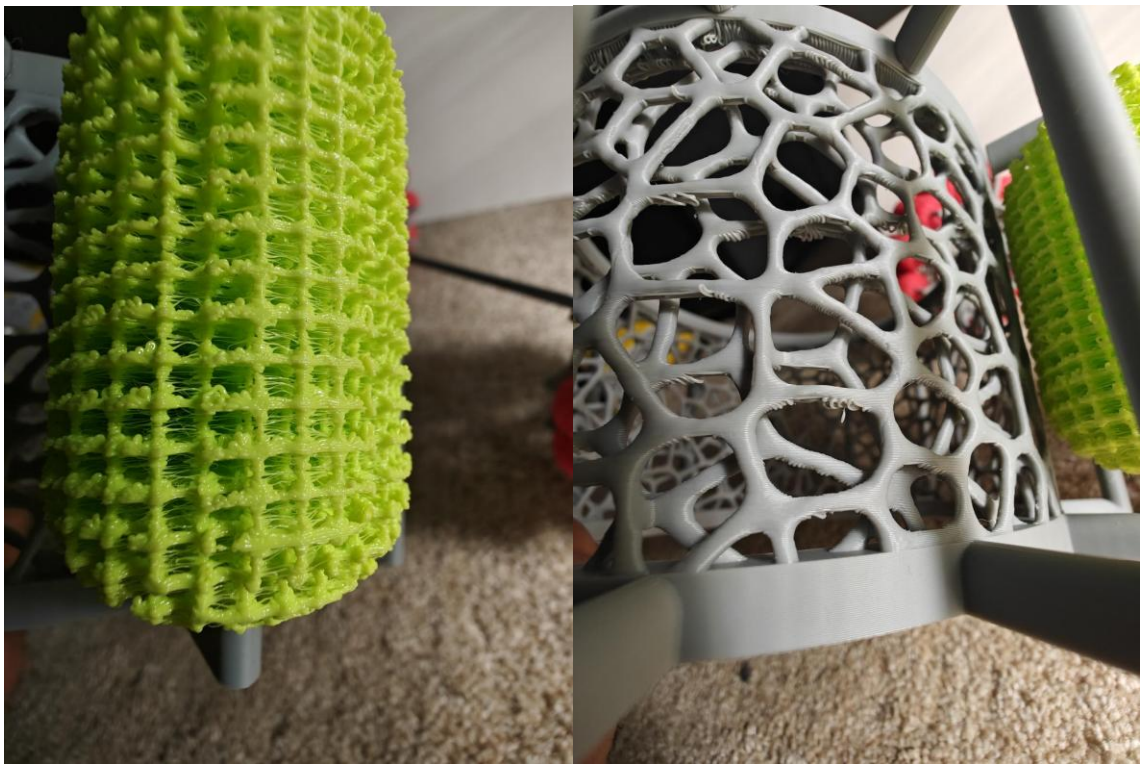

Figure 22: Left: Heavy stringing noticed in TPU parts; Right: Sagging seen in unsupported PLA lattice structures

D. Insights for Future Development

The printing trials provided strong qualitative validation of the wheel's manufacturability using accessible, low-cost AM technology. While scaled TPU components highlighted the geometric and material challenges associated with printing compliant features, full-size prototypes validated the design's assembly logic, modularity, and functional integrity. These insights will inform future refinements to the wheel's additive geometry and support the development of flight-capable configurations optimized for Martian deployment. This validation process demonstrated the practical feasibility of the modular wheel concept but also exposed critical limitations at reduced scales and in flexible materials. For flight or mission-grade implementation:

a. Higher durometer TPU (75D or greater) with additives for UV and thermal resilience would be necessary.
b. Larger tread modules should be redesigned with print-friendly wall angles and minimized overhangs to support in-situ manufacturing.
c. Multi-axis printers or dedicated TPU slicers may be needed to produce fine, deformable lattices without deformation or buckling.
d. Full-scale integration with CNC Ti parts will require precise interface calibration to accommodate AM variances and potential shrinkage.

VIII. Design Validation and Prototype Testing Results

A. FEA Analyses

To evaluate the structural response of the full-scale Octa-Hedroid tire lug under a wheel's normal load, we built a static finite-element model of the lug geometry (as depicted in Figure 23), including its internal lattice infill and central mounting bore. The TPU 75D material was defined as linear-elastic. A fine tetrahedral mesh (max element edge ~0.1 mm) was used throughout the struts and shell to accurately capture the lattice topology and stress concentrations at node junctions.

The **central bore** was treated as a rigid coupling surface: a uniform, downward-directed normal force (**equal to the wheel's design load - 64 kg per wheel**) was applied to all bore-inner nodes, simulating the compressive load transmitted from the hub. At the **lower end face** of the lug—the surface that interacts against the soil surface—a fully fixed boundary condition (all translations and rotations locked) replicates the contact patch interaction (due to computational limitations a contact surface could not be used as the computational time was excessively high . All other exterior faces were left free of constraint, isolating the investigation to the primary compressive scenario.

By combining this loading and support scheme with the detailed mesh, the analysis captures the maximum vertical deflection and von Mises stress distribution throughout the lattice (as depicted in Figure 24). These results directly inform both stiffness performance and the safety margin against yielding, guiding further scaling and optimization of strut diameter for the final tire lug design.

**Note: Due to computational limitations, a 4mm cut section of the lug geometry was used. The team expects to see consistent results (better) with the full model which is intended to perform when higher computational resources are available. (No. of Elements in full model is 2-3 million and the cut section has 10k elements)*

To validate our bench-scale findings in a more realistic geometry, we performed a full-scale FEA on a cut-section of the Octa-Hedroid tire lug, including its central mounting bore (**the vertical load was scaled down accordingly to 3 kg**). Unlike the small block used for initial benchmarking, this model captures the actual boundary conditions of a lug inserted into a wheel: a concentrated normal load at the bore and a fixed interface at the rim flange. The resulting displacement and stress fields (max U = 1.64 mm, max von-mises stress = 11.6 MPa) as depicted in Figure 24, differ significantly from the block test, reflecting key differences in structural connectivity and load path.

The cut-section lug deflects nearly three times more than the bench-block (1.64 mm vs. 0.57 mm) primarily because the cut section omits the continuous lattice "neighbors" that, in the block case, provided lateral support and constrained out-of-plane deformation. In the wheel lug, the side faces are free, so struts at the perimeter bend and twist unrestrained, adding compliance. Moreover, whereas the block test spreads the vertical load uniformly across an entire face, here the force is concentrated through the bore's small inner surface, amplifying local bending and overall deflection.

Although the peak von Mises stress (11.6 MPa) remains below TPU 75D's allowable, its pattern also reflects the cut geometry and load concentration. The absence of adjacent lattice cells at the edges removes stress "sharing" pathways, causing more pronounced stress gradients radiating from the bore. In contrast, our benchmark block exhibited a more uniform stress field because each node had full connectivity in all directions and loads were distributed. The single-bore load case therefore generates both local stress concentrations and wider compliance—even at a slightly lower absolute peak stress.

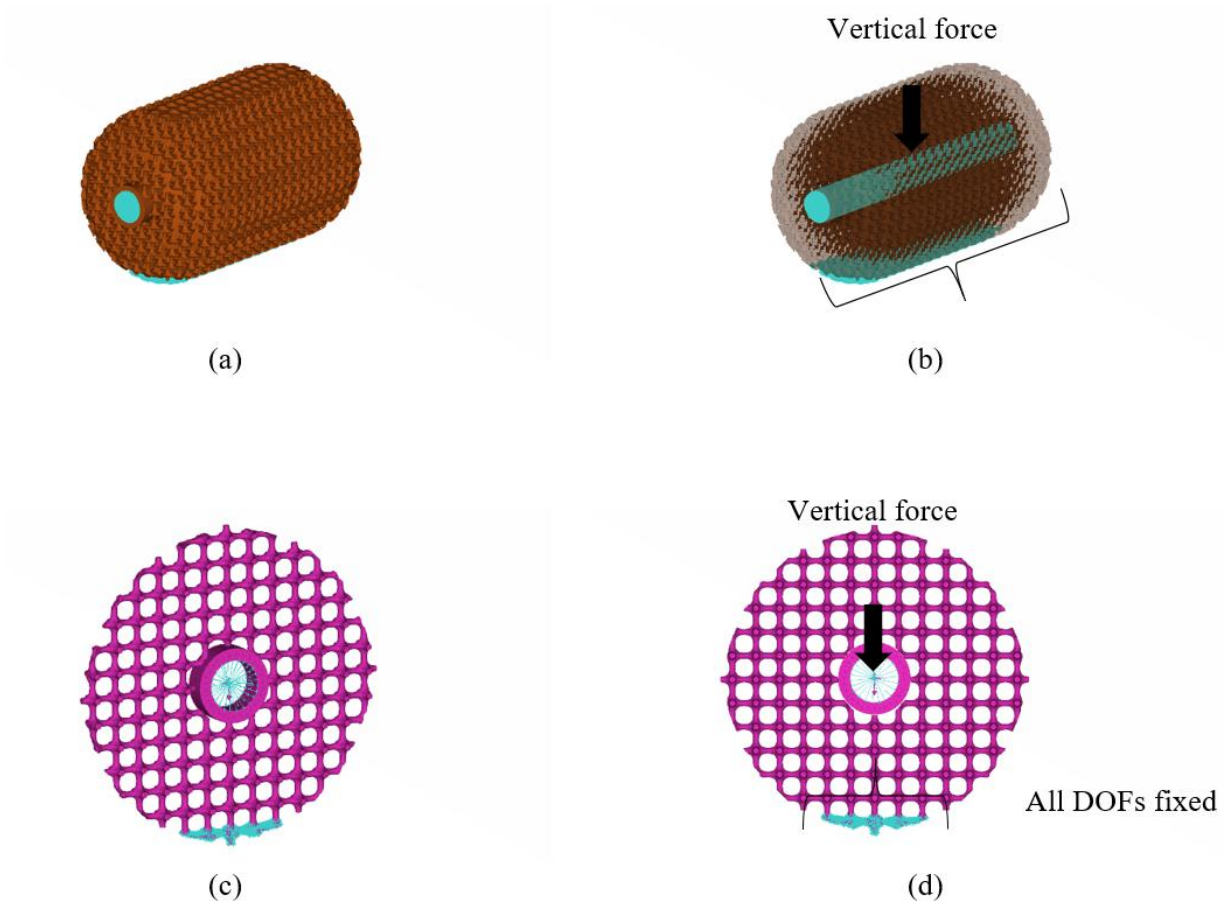

Figure 23: Finite Element Analysis Model Setup for tire lug

(a) Full model Mesh (b) Full model BC (c) Cut-section model Mesh (d) Cut-section model BC

These results underscore that a full-scale Octa-Hedroid lug modeled as an isolated cut-section exhibits larger deflections and altered stress patterns than our small, periodic block test (which showed ≈0.6 mm deflection), yet still lower stresses than the unconstrained slice model. In the cut-section, free edges allowed peripheral struts to bend and twist under the applied wheel load, producing a peak vertical deflection of 1.64 mm—even though von Mises stresses remained within the TPU 75D safety margin. Reinstating lateral support from all 21 repeating lattice slices in the complete lug will force compressive loads to distribute through multiple strut paths, reducing deflection back towards the ~0.6 mm benchmark and evening out stress concentrations.

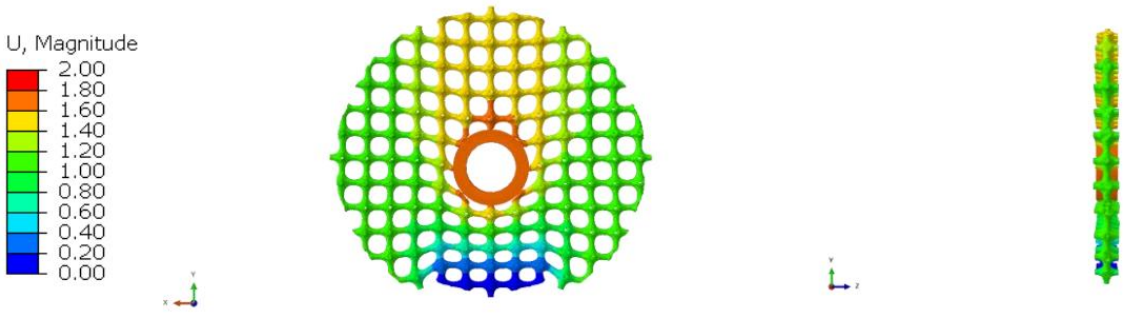

(a) Max Disp: 1.64 mm

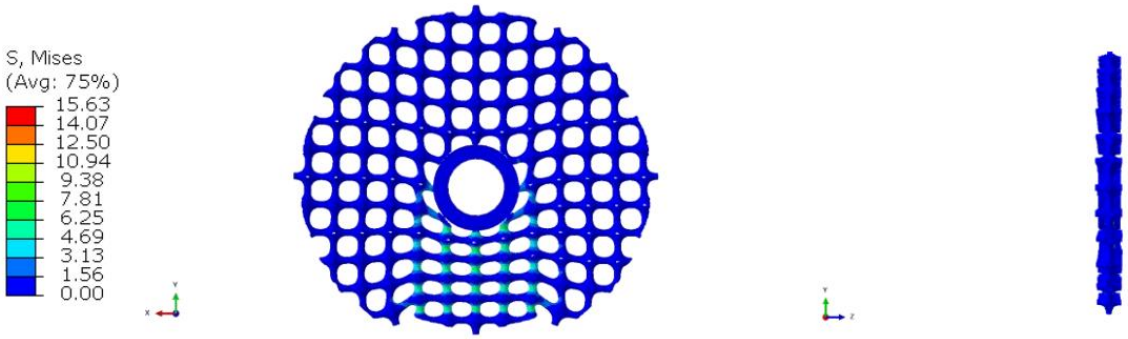

(b) Max Mises Stress: 11.61 MPa

Figure 24: (a) Deformation Plots for the Cut-Section model of tire lug (Front and Side View)

(b) Von-Mises Stress Plots for the Cut-Section model of tire lug (Front andSide View)

Likewise, the stress distribution in the complete lug will become far more uniform. In the cut-section model, stress concentrations radiated from the central bore into unconstrained neighbors, creating localized von Mises peaks up to 11.6 MPa. Once all cells are connected, those peak stresses will diffuse into a larger network of struts, evening out gradients and lowering hotspots to levels closer to the 15 MPa benchmark or below. Edge effects—where the absence of neighboring geometry produced bending risers—will vanish, ensuring that every node shares load symmetrically and maintains the safety margin built into the TPU 75D design.

In sum, by modeling the full-scale tire lug as a contiguous Octa-Hedroid lattice rather than an isolated slice, we recover both the stiffness and stress uniformity demonstrated in our idealized block study, while preserving the lattice's inherent self-cleaning channels. This confirms that the chosen topology scales favorably to prototypes, delivering the necessary load-bearing capacity and operational reliability for Martian terrain. To ensure sufficient stiffness under actual rover weights, we will increase strut diameter (or add a thin outer shell) while preserving the Octa-Hedroid's large, interconnected voids for debris egress.

B. TPU Lug Thermal Testing

To understand the preliminary potential temperature resilience and deformation response of the TPU tread modules in Martian-like or test-relevant conditions, a comparative thermal evaluation was conducted on two lugs fabricated at different scales. These lugs, printed in TPU 90A using a Bambu Lab P1P, represent the smallest modular element of the tread system and were selected for standalone analysis due to their complex geometry, flexibility, and exposure during rover operation. The goal was to observe how each lug reacts to common temperature extremes by placing them in two everyday conditions: Inside a **home freezer** (~ -15°C) for 20 minutes; Near a **warm heater vent** (~50–60°C surface temperature) for 15–20 minutes.

For the 1:2 Scale Lug:

- In the freezer, the smaller lug became noticeably stiff and lost most of its flexibility. It remained intact but felt brittle to the touch.
- Near the heater, it softened quickly and began to lose its shape, especially around the thinner lattice sections. Slight deformation remained even after cooling.
- This suggests that smaller TPU parts are more prone to heat-related shape changes and cold brittleness due to their thin walls and lower mass.

For the 1:1 Scale Lug:

- In the freezer, the full-size lug became firm but still flexible enough to bend without cracking.
- Near the heater, it remained stable. There was no visible warping, and it fully returned to shape after being lightly compressed by hand.
- The added mass and thicker wall sections helped it handle temperature changes much better.

Takeaways

a. Larger TPU lugs (1:1) are more reliable under temperature swings and hold their shape better.
b. Smaller TPU lugs are easier to print and test but are not suitable for structural use — they deform more easily with heat and stiffen too much when cold.
c. For Mars-like environments, stronger materials like TPU 75D with UV and cold resistance would be needed, but these quick tests helped confirm that our full-scale design holds up better, even with regular TPU 90A for Earth-based tests for initial prototypes.

C. Impact Resistance, Shock and Durability Testing

To evaluate the impact resilience and structural integrity of the Mars rover wheel prototype under conditions simulating sudden terrain drops or deployment impacts, a drop test was conducted using the fully fabricated 1:2 scale model (Figure 18). The test involved vertically releasing the prototype from an increasing height of 10cm to 100 cm onto a concrete surface, representative of a worst-case rigid terrain impact scenario. The prototype was dropped in two orientations: (1) vertically with the hub facing downward and (2) laterally such that the TPU lugs made primary contact with the surface. These orientations were chosen to simulate typical landing shocks and wheel-edge collisions experienced during rover deployment or traversal of rocky Martian outcrops.

Upon impact, the TPU lugs exhibited localized deformation but fully recovered to their original geometry, demonstrating excellent elastic resilience. No visible cracking, delamination, or interfacial disbonding was observed at the junction between the tread modules and the PLA rim. This performance supports the hypothesis that energy dissipation is efficiently managed by the compliant lug geometry and lattice infill design. Additionally, the PLA-based structural components remained mechanically intact, although minor cosmetic scuffing was noted on the rim edges, suggesting localized surface stress concentrations that would likely be mitigated in the full-scale titanium version.

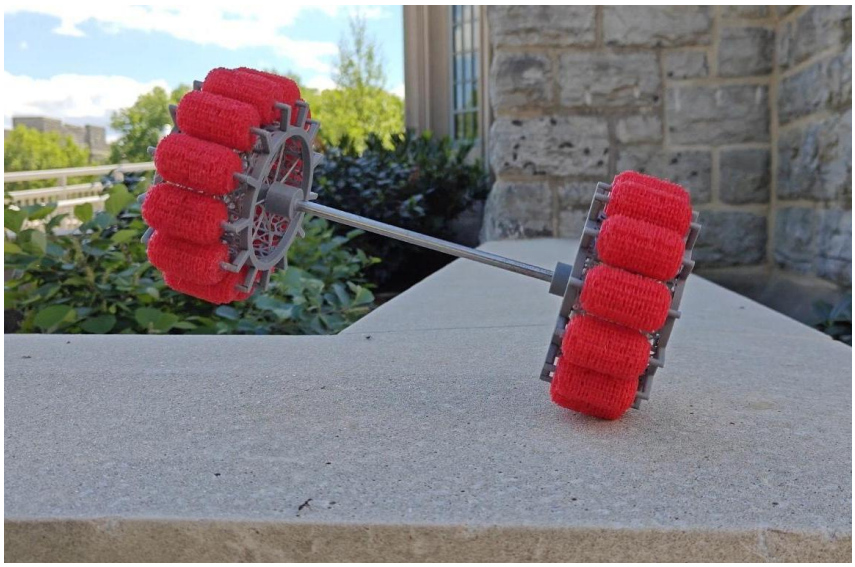

Figure 18: Drop Test of the fully fabricated prototype, from 1 m. height

Overall, this test supports the wheel's capability to absorb low- to moderate-energy shocks through a combination of compliant TPU elements and distributed structural reinforcement. While not instrumented with strain gauges or accelerometers, the test provides strong qualitative evidence that the final design is robust against drop-induced failures and supports the engineering rationale behind modular compliance and lattice-based impact mitigation in extraterrestrial rover applications.

D. Friction and Rolling Resistance Testing

To assess the terrain adaptability and locomotion efficiency of the final wheel design, a series of qualitative rolling resistance tests were conducted using the 1:2 scale fully assembled prototype. These tests were aimed at evaluating the wheel's passive rolling behavior under no-load conditions across three common terrestrial terrains: grass, gravel, and concrete. Each test was performed by manually pushing the wheel assembly along a flat surface and observing the degree of resistance, wheel deformation, and directional stability.

- Grass Terrain: On moderately thick grass, the wheels demonstrated notable resistance to rolling, primarily due to the elastic sinkage of the TPU lugs into the turf. However, the flexible lattice design of the lugs enabled gradual deformation, allowing them to conform to undulations in the grassy surface. This resulted in a slightly jerky but forward-moving roll, indicating good grip and traction but with increased energy expenditure. The wide contact patch of the cylindrical lugs minimized deep embedment, suggesting a beneficial balance between compliance and surface area for off-road terrains like Martian regolith analogs.

- Gravel Terrain: When tested over medium-grain loose gravel (5–15 mm granules), the wheel showed enhanced adaptability. The TPU lugs were able to dynamically deform and interlock with gravel elements, which prevented slippage and allowed for consistent forward motion. Rolling resistance remained moderate, as the protruding lugs avoided significant sinkage and dispersed the weight efficiently. Notably, the tangential orientation of the dowel-supported lugs helped prevent lateral slippage and promoted directional stability, a critical feature for uncertain Martian slopes and rocky plains.

- Concrete Terrain: On smooth concrete, the wheel exhibited low rolling resistance with minimal deformation of the TPU lugs. The rigid, flat surface enabled near-frictionless rolling, and the symmetric tread layout ensured directional stability and balanced motion. While concrete is not representative of Martian soil, this test served as a control to evaluate baseline performance. Importantly, the TPU lugs did not show excessive wear or flattening,

indicating that even under repeated rolling cycles, the 90A TPU maintains shape fidelity, critical for mission longevity.

These terrain-based evaluations affirm that the modular lattice-based TPU lugs contribute significantly to the wheel's multi-terrain performance. While grass induced the highest resistance and concrete the least, the design showed no critical failures or deformations in any condition. These tests reinforce the choice of compliant modular lugs and a skeletonized hub-lattice structure as an effective trade-off between traction, durability, and manufacturability.

E. Surface Contaminant Rejection and Regolith Shed Testing

One of the key environmental challenges for Mars surface systems is the accumulation of fine-grained regolith, which can reduce traction, interfere with mechanical joints, and degrade long-term performance. To address this, the final wheel design incorporated passive dust-repelling strategies, particularly in the geometry of the lugs and the overall part layout. While this study used PLA-based prototypes for structural elements in place of titanium (due to lab access and scope constraints), several observations were made about the dust-shedding behavior of the modular wheel in Earth-analog conditions.

The wheel's TPU 90A tread lugs, printed on the Bambu Lab P1P, feature macro-lattice infill patterns with high porosity and smooth cylindrical surfaces. This design was intended not only for compliance and traction but also for passive dust shedding. During test rolling over dusty, granular surfaces like garden soil and dry mulch (Figure 19), these TPU lugs demonstrated a tendency to expel debris from the lattice during compression and rebound cycles. The elasticity of TPU acted as a self-cleaning mechanism, causing soil to dislodge from the lattice voids as the wheel flexed during rotation. This supports the intended goal of regolith minimization without active sweeping systems.

The PLA-printed rim, hub, and support structures, while not representative of aerospace-grade titanium (as intended in final implementation), offered insights into surface geometry and gap tolerances that influence regolith accumulation. The printed PLA surfaces were not sealed or coated, leaving mild surface roughness that could trap fine dust. However, the lack of complex recesses and tight tolerance interfaces in the design helped minimize particle entrapment in joints and sockets. Despite repeated outdoor testing, no critical dust buildup or binding was observed at spoke-dowel interfaces or the lug mounting zones. It is worth noting that PLA lacks the anti-adhesion oxide layer or electrostatic neutrality of titanium, so any observed dust resistance at this prototyping stage represents a conservative performance estimate — the final titanium implementation would likely perform even better under real Martian conditions.

Real-World Testing Observations: Throughout rolling trials on gravel, dry soil, and dusty concrete, the wheel shed visible surface dust effectively, and no clumping or jamming occurred. Most collected debris was superficial and could be cleared with light brushing, validating the design's modular cleanliness and low-maintenance surface exposure. The open lattice tread design proved particularly helpful for dust ejection, further supporting its relevance for regolith-heavy environments.

Figure 19: Dust shedding test over a non-homogeneous surface consisting of organic matter, dust, and stones of varying sizes

F. Variable Inclination Traction Assessment

To evaluate the terrain adaptability and traction efficiency of the final wheel design, a series of qualitative traction tests were performed using the 1:2 scale prototype. These tests aimed to simulate real-world Martian-like terrain conditions by assessing the wheel's grip and deformation response on sloped, irregular, and fragmented surfaces. The tests incorporated both controlled incline boards and natural broken concrete structures found in construction zones on campus, representing realistic uneven terrain. The wheel was rolled and statically positioned on:

- Wooden incline boards (0°–30°)
- Rough sandpaper patches to simulate high-friction terrain
- Fractured concrete slabs with discontinuities, gaps, and varying elevation (mimicking Martian rocks or layered terrain)

Inclination angles were manually varied and measured using a digital angle finder. Observations focused on lug compression, surface contact, slipping tendency, and recovery after traversal.

Observations:

a. On controlled inclines (0°–20°): The wheel rolled smoothly with minimal slippage. TPU lugs compressed and adapted to the slope without significant deformation loss. On coarse textures, the cylindrical lugs conformed and held surface contact effectively.
b. On 25°–30° inclines: On smoother surfaces like plywood, the 1:2 scale lugs began to slide under their own weight. However, when rolling over sandpaper or gravel-covered boards, traction was retained due to localized deformation and texture interlock.

c. On broken concrete terrain: When tested over cracked concrete slabs with irregular elevation (~5–10 cm gaps), the wheel exhibited impressive passive adaptability. TPU lugs flexed into gaps, bridging voids and gripping sharp edges without tearing or detachment. The cylindrical profile allowed for partial contact even on angled segments, and the flexible lattice acted like a passive suspension system. (Figure 20)

d. Failure Mode: On vertical ledges or continuous sharp edge transitions (>30° height differential), the wheel was unable to climb or retain grip, especially at low mass. However, no permanent damage or material fatigue was observed in the PLA frame or TPU lugs.

Figure 20: Prototype wheel being tested on broken concrete slabs and structures. Modular TPU lugs offered consistent grip across slope gradients and irregular textures, supporting the intended use case of Martian surface mobility where regolith, rock fragments, and slopes interact unpredictably.

These tests confirmed that the wheel's lug deformation, modular traction geometry, and part flexibility allow it to traverse uneven and moderately inclined terrain effectively. The broken concrete test in particular validated the wheel's ability to conform to real-world, discontinuous terrain with performance strongly governed by lug geometry and material compliance. Though scaling effects limited the load and deformation depth, results suggest significantly improved behavior at full scale (1:1), where greater mass and tread area would enhance grip.

IX. Cost Analysis

To capture the full economic picture of our Mars rover wheel development, we evaluated four distinct build stages—1:1 desktop prototyping, 2:1 (or 5:1) scaled structural prototyping, full-scale aerospace prototype, and flight-ready Martian deployment unit. For each stage we separately estimated material costs (from PLA/TPU filaments up to space-grade Ti-6Al-4V powders and certified components) and manufacturing costs (ranging from basic printer run-time and electricity through LPBF, CNC, HIP, and NASA-level qualification). The resulting total-cost ranges—from under $20 for a low-fidelity desktop print, to $1.4–3.5 k for a hardware-validated scale model, to $8–15 k for a functionally accurate aerospace prototype, and up to $70–150 k for a fully certified Mars-ready unit—reflect both the raw build expenses and the escalating overhead of post-processing, inspection, and qualification.

We evaluated cost across four stages: desktop prototyping, industrial-scale prototyping, full-scale aerospace testing, and Martian deployment. The 1:1 desktop prototype, printed with PLA and TPU on a Bambu Lab P1S, cost under $20 in material and print time. Scaled prototypes using aerospace-grade materials such as Ti-6Al-4V and TPU 75D—fabricated via LPBF and CNC—are estimated at $1,400–$3,500, reflecting the increased complexity and precision required.

A full-scale functional prototype with post-processing, heat treatment, and structural validation is expected to cost $8,000–$15,000. For a flight-ready Martian unit, which includes qualification testing and redundancy, costs could exceed $70,000.

All estimates are summarized in Table 6 and reflect vendor-based pricing. Capital equipment costs are excluded, as LPBF and CNC processes are assumed to be outsourced to certified aerospace manufacturers to ensure compliance with required precision and material standards.

Table 9: Cost Estimation of Prototypes and Final Product

Type	Material Cost Estimate	Manufacturing Cost Estimate	Total Cost Range	Notes
1:1 Desktop Prototype	$3–8 (PLA + TPU 90A filament) [12]	$0–10 (printer usage/electricity) [12]	$13-18	Low-fidelity visual/proof of concept prototype for quick iteration using minimal filament.
2:1 or 5:1 Scale Prototype	$400–1,000 (Ti-6Al-4V + TPU 75D) [18]	$1,000–2,500 (LPBF + CNC machining + ME) [18][19]	$1,400-3,500	Scaled prototype with realistic structural performance; used for experimental validation.
Full-Scale Aerospace Prototype	$3,000–5,000 (Ti alloy, TPU, post-processing) [18][19]	$5,000–10,000 (incl. LPBF, HIP, CNC, QC) [18][19]	$8,000-15,000	Functionally accurate version; includes heat treatment, machining precision, and subsystem integration.
Flight-Ready Martian Deployment Unit	$20,000–50,000+ (space-grade materials, QA, cert., assembly) [20][21]	$50,000–100,000+ (NASA flight qualification tier) [20][21]	$70,000-150,000	Fully tested and certified unit for Martian deployment, including environmental testing and redundancy.

This tiered cost breakdown highlights two key insights: first, while desktop prototyping is effectively "pocket-change" in materials and run-time, true lab-rate and labor overhead drive its real cost into the low-tens of dollars; second, once aerospace-grade performance, heat-treatment, high-precision machining, and flight qualification enter the picture, certification and skilled labor become the dominant cost drivers—easily eclipsing raw AM build expenses by 3–5×. These findings underline the importance of carefully balancing prototype fidelity against budget constraints and suggest that streamlining post-processing protocols or leveraging lower-cost qualification pathways could dramatically reduce the cost of future high-performance AM components.

To comprehensively understand the investment required for our Mars rover wheel concept, we conducted two parallel cost studies: one for a 1:1 desktop-scale prototype produced on a Bambu Lab P1S using PLA and TPU, and another for a flight-like aerospace prototype incorporating Ti-6Al-4V lattices (LPBF), CNC-machined hubs and rims, post-processing (HIP, finishing), and TPU treads. In each case, we captured both direct expenses—material, machine time, consumables—and indirect expenses—labor for setup, support removal, inspection, overhead, and, in the aerospace case, rigorous qualification testing. This approach ensures that our cost estimates move beyond "raw" material and energy Figures to reflect true laboratory and vendor rates, revealing the real economic footprint of prototyping versus full-scale production.

Table 10: 1:1 Desktop Prototype Cost Study

Cost Element	Assumption	Cost (USD)
PLA filament	0.05 kg @ $25/kg	$1.25
TPU filament	0.03 kg @ $25/kg	$0.75
Print time (Bambu P1S)	0.5 h @ $10/h	$5.00
Electricity	0.1 kWh @ $0.12/kWh	$0.01
Support removal & cleanup	0.25 h @ $30/h	$7.50
Setup & post-proc labor	0.25 h @ $40/h	$10.00
Consumables & wear	Nozzle, build-tape prorated	$2.00
Overhead (10 %)	On all above	$2.35
Total		**$29. 86**

Notes: Material + print time alone runs under $7, but adding labor & overhead brings the real cost to ~$30. This explains why rough "under $20" estimates (material + energy only) often understate true prototyping effort.

Table 11: Full-Scale Aerospace Prototype Cost Study

Cost Element	Assumption	Cost (USD)
Ti-6Al-4V powder	0.3 kg @ $150/kg	$45.00
Additional support powder	0.1 kg @ $150/kg	$15.00
LPBF machine time	15 h @ $80/h	$1,200.00
Hot-Isostatic Press (HIP)	Single cycle, external vendor	$300.00
CNC machining (hub, rim, ribs)	10 h @ $250/h	$2,500.00
Surface finishing (blasting, polish)	5 h @ $100/h	$500.00
Quality control & inspection	4 h @ $150/h	$600.00

TPU tread modules (FDM)	0.2 kg @ $25/kg	$5.00
FDM machine time	2 h @ $10/h	$20.00
Assembly & fixturing labor	4 h @ $50/h	$200.00
Certification & qualification tests	Environmental, fatigue, redundancy (NASA-tier)	$5,000.00
Project overhead (15 %)	On all direct costs	**$1,442.25**
	Total	**$11,827.25**

Notes: Direct manufacturing (powder, AM, CNC, post-proc) comes to about $5.1 k. Adding flight-qualification testing (~$5 k) and overhead pushes the total to ~$12 k—which is within your $8–15 k range . This detailed study reveals that certification and labor dominate costs; powder and machine time are a surprisingly small fraction of the total.

The detailed breakdown underscores a critical insight: while desktop prototyping remains economically accessible (≈$30 per wheel) when accounting for labor and overhead, aerospace-grade prototypes incur substantially higher costs, driven chiefly by certification, finishing, and skilled-labor requirements (≈$12 k per wheel). Powder and machine time—often assumed to dominate additive-manufacturing budgets—actually represent a modest fraction of the total. Instead, post-processing, quality assurance, and flight-qualification testing emerge as the most significant cost drivers. These findings highlight opportunities to streamline future iterations—for example, by optimizing qualification protocols or leveraging emerging near-net-shape processes—to bring high-performance, AM-enabled rover wheels within a more sustainable budget envelope.

X. Limitations and Future Recommendations

A. Current Work Limitations

Despite the encouraging performance trends observed in our bench-scale and cut-section analyses, several constraints temper the generality of these results. First, all FEA simulations treated TPU 75D as a linear elastic material, omitting its true viscoelastic, hysteretic, and fatigue behavior under repeated loading. The cut-section model further simplified boundary conditions by excluding soil–tire contact, frictional interactions, and environmental effects such as thermal cycling and vacuum exposure, which are critical for accurate predictions of traction, sinkage, and material aging on Mars. Prototype validation relied on desktop-scale prints in PLA and TPU 90A, whose mechanical properties and scale-dependent phenomena (warping, brittleness) differ substantially from full-scale Ti–TPU assemblies. On the manufacturing side, fine lattice features encountered warping, stringing, and uneven surface roughness, raising concerns about dust entrapment and long-term integrity. Our cost analysis, although detailed across prototyping through flight-qualification phases, excluded capital expenditures and facility overhead, and is sensitive to vendor-specific pricing variability and certification protocols (±30%). Finally, the current study focused solely on static normal loading; dynamic, multiaxial, fatigue, and abrasive wear effects—integral to real rover operations—remain to be rigorously evaluated.

B. Future Work and Recommendations

To further advance this design towards flight-ready hardware, several avenues should be pursued. First, a parametric optimization of unit-cell size and strut diameter under varying compressive and cyclic loads will identify the minimum material usage that still meets stiffness and durability requirements. Next, integrated soil–tire interaction simulations (e.g. SPH or discrete element methods coupled with FEA) should be performed to validate traction, sinkage, and the self-cleaning behavior of the Octa-Hedroid lattice on realistic Martian regolith analogs. Experimental prototyping—printing full-scale lugs and testing them in a regolith chamber—will then confirm model predictions and reveal any printability or fatigue issues. Additionally, further testing can be implemented using other particle types

like ARD (Arizona Road Dust, CSPEC, etc.) [22], which can help understand the design aspects and help modify the current design for on-Earth terrestrial uses also. Finally, future simulations of the complete wheel assembly—with rim constraints and full lattice continuity—will finalize strut sizing and outer shell thickness, ensuring the tire lugs deliver the required load-bearing capacity, longevity, and debris-egress performance for mission-ready deployment.

XI. Conclusion

This research presents a novel, hybrid-manufactured Mars rover wheel designed explicitly to address the inherent limitations of existing rigid metallic wheels and pneumatic terrestrial tires for extraterrestrial applications. By strategically integrating a CNC-machined titanium framework, LPBF-printed titanium lattice structures, and ME-printed modular TPU tread lugs, the developed wheel distinctly combines structural resilience, terrain adaptability, and modular maintainability—features uniquely suited to the demanding Martian environment.

The primary novelty of this work lies in the meticulous design and validation of a flexible lattice-based modular tire, employing a specialized Octa-Hedroid lattice topology within TPU 75D tread lugs. This topology offers superior stiffness-to-weight characteristics, uniform stress distribution, and optimized regolith shedding capabilities compared to conventional lattice structures, directly translating to enhanced durability and operational reliability on abrasive Martian terrain. Moreover, the modular replaceability of individual TPU tread components dramatically improves mission longevity and reduces maintenance logistics, which are critical for sustained rover mobility far from Earth-based support systems.

Comprehensive finite-element analyses and practical validation tests—including impact resistance, rolling friction, and thermal stability—demonstrated the wheel's excellent mechanical performance and adaptability across diverse terrestrial analog terrains, reinforcing its suitability for future extraterrestrial exploration missions. Although prototype evaluations revealed manufacturing challenges associated with scale and material selection, these limitations represent critical insights rather than fundamental barriers. Specifically, future material refinement with TPU 75D incorporating UV-resistant, anti-static, and cryogenically stable additives will further enhance the wheel's robustness and mission-readiness. Overall, this innovative hybrid manufacturing approach not only surpasses traditional rover wheel designs in adaptability, repairability, and performance efficiency, but also establishes a robust platform for future advancements in additive manufacturing for planetary exploration. The outcomes of this study provide a foundational blueprint and compelling rationale for adopting flexible, lattice-structured wheels in upcoming Mars missions, significantly advancing the capabilities and durability of rover mobility systems for exploration of challenging extraterrestrial terrains.

Acknowledgments

The team would like to express sincere gratitude to Dr. Jan Helge Bøhn for his invaluable guidance, insightful feedback, and continuous support throughout the course of this project. His expertise in additive manufacturing and rapid prototyping greatly enriched our understanding and played a pivotal role in shaping the direction and execution of this work.

References

[1] California Institute of Technology, “Mars 2020 Perseverance Landing Press Kit,” NASA Jet Propulsion Laboratory, https://www.jpl.nasa.gov/news/press_kits/mars_2020/landing/mission/spacecraft/perseverance_rover/ (accessed May 6, 2025).

[2] Lakdawalla, Emily. "Diagram of a Curiosity Wheel." The Planetary Society, 2012, https://www.planetary.org/space-images/diagram-of-a-curiosity-wheel.

[3] NASA. Break in Raised Tread on Curiosity Wheel. NASA Science, 21 Mar. 2017, https://science.nasa.gov/resource/break-in-raised-tread-on-curiosity-wheel. Accessed 6 May 2025.

[4] Williams, David R. “Mars Fact Sheet”. NASA Goddard Space Flight Center, 23 Oct. 2024, https://nssdc.gsfc.nasa.gov/planetary/factsheet/marsfact.html. Accessed 6 May 2025.

[5] Kilkenny, Nancy Smith. "Reinventing the Wheel." NASA, 26 Oct. 2017, https://www.nasa.gov/specials/wheels/. (accessed May 6, 2025)

[6] Lubrizol. “Pellethane ® 2363 Series TPU.” Lubrizol Life Science, 2024. https://www.lubrizol.com/-/media/Lubrizol/Health/TDS/Pellethane-2363-Series-TPU-TDS.pdf (accessed May 6, 2025)

[7] Cheetah Precision. What Is the Tightest Tolerance for a Precision Machining Company? Cheetah Precision, https://www.cheetahprecision.com/what-is-the-tightest-tolerance-for-a-precision-machining-company. Accessed 6 May 2025.

[8] Kyocera SGS Europe. "Titanium Properties." Kyocera SGS Europe, https://kyocera-sgstool.co.uk/titanium-resources/titanium-information-everything-you-need-to-know/titanium-properties/. Accessed 6 May 2025.

[9] Calculating the price of 3D printing technologies: A comprehensive analysis of SLS, SLA, SLM, MJF, FDM, and more. (n.d.). 3D Printing.

[10] Cao, S., Zou, Y., Lim, C. V. S., & Wu, X. (2021). Review of laser powder bed fusion (LPBF) fabricated Ti-6Al-4V: process, post-process treatment, microstructure, and property. Light: Advanced Manufacturing, 2(3), 313-332.

[11] "Advancing Industries with High-Performance TPU Solutions." Covestro, Apr. 2025, https://solutions.covestro.com/-/media/covestro/solution-center/digital-event-space/pu-india/tpu-brochure--putech-india.pdf. Accessed 6 May 2025.

[12] Ultimaker, “S5 Technical Specifications” UltiMaker, https://ultimaker.com/3d-printers/s5. Accessed 7 May 2025.

[13] Markforged. (2025, April 18). FX20TM. https://markforged.com/3d-printers/fx20-2

[14] EOS M 400 - Mid-Size 3D Printing. (n.d.). EOS GmbH. https://www.eos.info/metal-solutions/metal-printers/eos-m-400#key-features

[15] AM400. (n.d.). Tech-Labs. https://tech-labs.com/products/am400

[16] Gibson, Lorna J. "ASHBY. MF Cellular solids Structure and properties." Edition: Cambridge Solid State Science Series. (1997).

[17] www.matweb.com/search/datasheet_print.aspx?matguid=58712e76ddbf45c5b7075ed490dd5c25.

[18] EOS, “GmbH. EOS M 400: Metal 3D Printer for Industrial Applications.” https://www.eos.info/metal-solutions/metal-printers/eos-m-400. Accessed 7 May 2025.

[19] Lubrizol, “Pellethane® 2363 Series TPU Technical Data Sheet,” Lubrizol Life Science, 2024, https://www.lubrizol.com/-/media/Lubrizol/Health/TDS/Pellethane-2363-Series-TPU-TDS.pdf. Accessed 7 May 2025.

[20] NASA, “Reinventing the Wheel.” NASA, 26 Oct. 2017, https://www.nasa.gov/specials/wheels/. Accessed 7 May 2025.

[21] Cheetah Precision, “What Is the Tightest Tolerance for a Precision Machining Company?” https://www.cheetahprecision.com/what-is-the-tightest-tolerance-for-a-precision-machining-company. Accessed 7 May 2025.

[22] Kurian, J., Patel, P. V., Lowe, K. T., & Ng, W. (2025). Particle Separation Efficiency in Canonical Vortex Tube Separator Arrays. In AIAA SCITECH 2025 Forum (p. 2109).